Inflammation favors the emergence of ETV6-RUNX1-positive pre-leukemic cells in a model of mesenchymal niche

Linda Beneforti[1], Erica Dander[1], Silvia Bresolin[2], Clara Bueno[3], Anthony Ford[6], Bernardt Gentner[7], Geertruy te Kronnie[2], Patrizia Vergani[8], Pablo Menéndez[3,4,5], Andrea Biondi[1,9], Giovanna D'Amico[1], Chiara Palmi[1*], Giovanni Cazzaniga[1*].

*C.P. and G.C. contributed equally to this work

1. Centro Ricerca Tettamanti, University of Milano-Bicocca, MBBM Foundation, Monza, Italy.

2. Dipartimento della Salute della Donna e del Bambino, University of Padua, Padua, Italy.

3. Josep Carreras Leukemia Research Institute, Department of Biomedicine, School of Medicine, University of Barcelona, Barcelona, Spain.

4. Institució Catalana de Recerca i Estudis Avançats (ICREA), Barcelona, Spain.

5. Centro de Investigación Biomédica en Red de Cáncer (CIBER-ONC), ISCIII, Barcelona, Spain.

6. Centre for Evolution and Cancer, The Institute of Cancer Research, London, UK.

7. San Raffaele Telethon Institute for Gene Therapy (SR-TIGET), IRCCS San Raffaele Scientific Institute, Milan, Italy.

8. Dipartimento di Ostetricia, MBBM Foundation, Monza, Italy.

9. Clinica Pediatrica, MBBM Foundation, University of Milano-Bicocca, Monza, Italy.

RUNNING TITLE: Inflammation favors E/R$^+$ pre-leukemia in the niche

CORRESPONDING AUTHORS

Giovanni Cazzaniga

Centro Ricerca M. Tettamanti, Pediatric Clinic, University of Milano Bicocca, MBBM Foundation, Monza, Italy.

Via Pergolesi, 33, 20900 Monza (MB), Italy.

E-mail: gianni.cazzaniga@asst-monza.it

Tel: +39 (0)39 2333661

Fax: +39 (0)39 2332167

and

Chiara Palmi

Centro Ricerca M. Tettamanti, Paediatric Clinic, University of Milano Bicocca, MBBM Foundation, Monza, Italy.

Via Pergolesi, 33, 20900 Monza (MB), Italy.

E-Mail: c.palmi@asst-monza.it

Tel: +39 (0)39 2332229

Fax: +39 (0)39 2332167

AUTHORS' DISCLOSURES OF POTENTIAL CONFLICTS OF INTEREST

There are no conflicts of interest to disclose.

Abstract

ETV6-RUNX1 (E/R) fusion gene, arising *in utero* from t(12;21), is the most frequent alteration in childhood acute lymphoblastic leukemia (ALL). Despite this, E/R is insufficient to overt disease since it generates a clinically silent pre-leukemic clone which contributes to hematopoiesis but fail to out-compete normal hematopoietic progenitors. Conversely, pre-leukemic cells show increased susceptibility to malignant transformation following additional genetic insults. Infections/inflammation are the most accredited triggers for mutations accumulation and progression in E/R^+ pre-leukemic cells. However, how E/R and inflammation interact in promoting leukemia, both directly or through other cellular components in the bone marrow (BM) niche, is still poorly understood. Here, we demonstrate that IL6/TNFα/ILβ pro-inflammatory cytokines cooperate with BM-MSC in promoting the emergence of E/R^+ murine pro-B cells over their normal counterparts by differentially affecting their proliferation, survival and migration. Very interesting, E/R-expressing human $CD34^+IL7R^+$ progenitors, a candidate population for pre-leukemic initiation during development, were preserved within the inflamed niche compared to their normal counterparts. Finally, the extent of DNA damage and activation-induced cytidine deaminase (AID) expression increase within the inflamed niche in both cell type, potentially leading to transformation in the apoptosis-resistant pre-leukemic clone. Overall, our data provide new mechanistic insights in childhood ALL pathogenesis.

Introduction

ETV6-RUNX1 (E/R), generated from translocation t(12;21)(p13;q22)(1,2), is the most frequent fusion gene in pediatric cancer (3), exclusively leading to B-cell precursors acute lymphoblastic leukemia (BCP-ALL) (4). Translocation occurs *in utero* in 2-5% of healthy newborns (5–7) and drives the expansion of a clinically silent pre-leukemic clone which contributes to hematopoiesis but fail to out-compete the normal counterpart, demonstrating the weak oncogenic potential of E/R (8–10). On the other hand, pre-leukemic cells show increased susceptibility to transformation following additional genetic insults, leading to overt disease in about 1% of E/R carriers (3,11).

While the biology of E/R^+ leukemia has been widely investigated, less is known about pre-leukemia. This is particularly important for the disease management if we consider that pre-leukemic mechanisms are responsible not only for the onset but also for long-term relapses evolving from secondary mutation in the original, chemoresistant pre-leukemic clone (12–15). Epidemiological and experimental data showed that infections and inflammation are the most accredited triggers for mutation acquisition and malignant progression in E/R^+ cells (16–20). Regarding this, we previously showed that E/R-expressing Ba/F3 cells are resistant to the antiproliferative effect of TGFβ, a pleiotropic cytokine produced under inflammation, thus facilitating the expansion of the pre-leukemic clone in competitive growth assays (21). Fittingly, TGFβ increased the absolute number of a candidate population of pre-leukemic stem cells from E/R-transduced human cord-blood (UCB) $CD34^+$ progenitors (21). More recently, it has been demonstrated that LPS exposure cooperated with AID and RAG1/2 enzymes to induce genomic instability in E/R pre-leukemic cells leading to leukemia in mice (19,22), while Sca1-E/R transgenic mice developed BCP-ALL at low penetrance only when exposed to common murine infective agents through increased RAG1/2 activity (ref. 19 and A.M. Ford, unpublished

observations). Overall, these observations seem to define a scenario in which infections and inflammation might prompt disease by *both* activating mutagenic mechanisms into pre-leukemic cells (16–20) and selectively expanding them in the bone marrow (BM) niche by altering the local microenvironment (23–25). It is well known, in fact, that hematopoietic stem-progenitor cells (HSPC) are strictly regulated by BM-derived signals both under physiological and pathological conditions. Of note, we previously suggested that E/R$^+$ could affect interactions of pre-leukemic cells with the BM niche because of their altered expression of key adhesion molecules and impaired migration towards CXCL12 (26). Recently, BM-mesenchymal stromal cells (MSC) have gained great interest as components of the niche for their active role in leukemia onset and progression (27–31). BM-MSC, for example, are stimulated by BCP-ALL blasts to secrete CXCR1/2-binding chemokines which attract leukemic but not normal progenitors, leading to the establishment of a self-reinforcing leukemic niche (32,33). Moreover, since they are able to sense and modulate inflammation, especially through the secretion of cytokines (34), BM-MSC can contribute to ALL pathogenesis (35,36). Regarding this, Zambetti et al. showed that, in leukemia-predisposing syndromes, mesenchymal-derived inflammation induces genotoxic stress in pre-leukemic HSPC favoring their progression to acute myeloid leukemia (AML) through the secretion of S100A8/9 (37).

Taking advantage of two E/R-expressing cellular systems (i.e. the murine pro-B cell line Ba/F3, a well-established inducible pre-leukemic model that we and others have successfully used in the past (21,26,38,39), and human umbilical cord blood (UCB)-derived CD34$^+$ progenitors), we show that BM-MSC and inflammation cooperate in favoring the emergence of E/R$^+$ pre-leukemic cells, in addition to predispose them to malignant transformation.

Material and methods

- **E/R-inducible Ba/F3 model**

The mifepristone-inducible GeneSwitch system (Life Technologies, Carlsbad, CA, USA) was used to express E/R, fused to the V5 epitope, in the IL3-dependent murine pro-B cell line Ba/F3. Cell viability and E/R expression efficiency were verified by flow cytometry using a FITC-conjugated anti-V5 antibody (Abcam, Cambridge, UK) as previously described. Experiments were performed with cells showing >85% viability and >80% FITC positivity except when specified in the text.

- **BM-MSC derivation and culture**

Murine and human healthy donors-derived BM-MSC were isolated and characterized as described in Supplementary Materials. Enrolled healthy donors were stem cell-donors whose BM was collected at the Pediatric Department of Fondazione MBBM/San Gerardo Hospital (Monza, Italy) for transplant purposes.

- **Competitive murine mesenchymal niche model**

Control and E/R^+ Ba/F3 were mixed ($2.5x10^4$ total cells) at a starting ratio of 20:80% and plated in standard liquid culture conditions in the absence (basal) or presence of rhTGFβ1 (10ng/mL) (R&D System), rmCXCL1 (100-500 ng/ml) or a cocktail of pro-inflammatory cytokines (20ng/mL rmIL6, 25ng/mL rmIL1β and 50ng/mL rmTNFα). Alternatively, cells were plated on murine BM-MSC in the presence or absence of inflammatory cytokines or LPS (InvivoGen, San Diego, CA, USA). In some experiments, mixed Ba/F3 cells were plated directly on BM-MSC or on a Transwells® insert of 0.4µm above BM-MSC. Where indicated, the CXCR2 inhibitor SB265610 was added (1µM). After 4 days of cultures, cells were analyzed as described in Supplementary Materials.

- **Ba/F3 gene expression profile**

E/R induction experiments in Ba/F3 showing >90% vitality and >90% FITC positivity were chosen for gene expression profile analysis by Gene Chip Mouse 2.0 Arrays (Affymetrix Inc., Santa Clara, CA, USA). Details are described in Supplementary Materials and **Supplementary Table S1**.

- **Migration assay**

Control and E/R^+ Ba/F3 ($3x10^5$) were resuspended in 100 µL of migration medium (Advanced RPMI, (Thermo Fisher Scientific, Waltham, MA, USA), 2% FBS (GE Healthcare), 1% L-glutamine (Euroclone, Milan, Italy) and loaded into the upper chamber of 8.0 µm Transwells (Costar Transwell® Permeable Supports, Corning Inc., MA, USA). Murine BM-MSC supernatant (600 µl) was added to the lower chamber. SB-265610 (Calbiochem, San Diego, CA, USA) (1µM) was used to inhibit CXCR2. The details can be found in Supplementary Materials.

- **Cell cycle analysis**

Control and E/R^+ Ba/F3 ($0.5x10^6$) were stained with 2.5µM carboxyfluorescein succinimidyl ester (CFSE) (eBioscience). $2.5x10^4$ stained cells were mixed (20%ctr:80%E/R^+) and cultured in 6-well plates under basal condition or on murine BM-MSC in the presence or absence of inflammatory cytokines. After 4 days, cells were analyzed by flow cytometry to determine CFSE mean fluorescence intensity (MFI). Details in Supplementary Materials.

- **Apoptosis and DNA damaging assays**

Mixed control (ctr) and E/R$^+$ Ba/F3 cells (20% ctr: 80% E/R$^+$, 2.5x10^4 tot) were cultured in 6-well plates under basal condition or on BM-MSC in the presence or absence of inflammatory cytokines. After 4 days, cells were analyzed by flow cytometry to determine the percentage of annexin V-negative E/R$^+$ or control Ba/F3 cells. Alexa Fluor® 647-anti-Phospho-Histone H2A.X Ser139 (20E3) (Cell Signalling, Danvers, MA, USA) MFI was used as indicator of DNA double strand breaks (DSB). Experimental details in Supplementary Materials.

- **Transduced UCB-CD34$^+$ and BM-MSC co-cultures**

Sorted pRRL-GFP and pRRL-E/R-GFP-transduced UCB-CD34$^+$ cells (see Supplementary Materials for details) were resuspended in stem culture medium (StemSpam SFEM-II, StemCell Technologies, Vancouver, Canada supplemented with 100 ng/mL SCF, 100 ng/mL FLT3-ligand, 10 ng/mL IL3, 20ng/mL IL6 and 50ng/mL TPO, all from Peprotech, Rocky Hill, NJ, USA)) and plated on BM-MSC monolayers in presence or absence of rhIL6 (40 ng/mL), rhIL1β (50 ng/mL) and rhTNFα (100 ng/mL) (Immunotools) for 72 h. At the end of the co-culture, cells were analyzed as described in Supplementary Materials.

- **Statistical Analysis**

Student's *t*-test with $p<0.05$ was used to define statistically significant results. Where indicated, one-sample *t*-test was used with the same significance threshold. Raw data were elaborated by Microsoft Excel or GraphPad programs.

Results

Inflammation favors the emergence of the E/R$^+$ pre-leukemic clone in an *in vitro* model of competitive mesenchymal niche

In order to investigate if BM-MSC and inflammation could cooperate in favoring the emergence of E/R$^+$ pre-leukemic cells, we performed a competitive growth assay as we did in the past to study the effect of TGFβ (21). In this assay, E/R-expressing (E/R$^+$) and control Ba/F3 cells are mixed at a starting ratio of 80%:20%, in consideration of the proliferative disadvantage of the first, and the mix is cultured for 4 days in presence or absence of candidate factors. In this case, the mix was plated on murine BM-MSC monolayers (a system indicated hereafter as “competitive mesenchymal niche”) with or without IL6, IL1β, and TNFα **(Supplementary Fig. 1)**. In agreement with our previous findings, we observed a substantial reduction in the percentage of E/R$^+$ Ba/F3 cells after 96h of standard liquid culture compared to day zero (28%±14% E/R$^+$). On the contrary, E/R$^+$ cells achieved a numerical parity with control cells in presence of TGFβ (50%±20% E/R$^+$, *p<0.01*) (21). Co-culturing E/R$^+$ and control Ba/F3 cells on unstimulated BM-MSC did not provide differences compared to basal condition (21%±12 % E/R$^+$, *p=ns*) while, interestingly, the addition of pro-inflammatory cytokines to the competitive mesenchymal niche significantly increased the percentage of E/R$^+$ Ba/F3 cells (47%±17% E/R$^+$, *p<0.01*) within the mix. Of note, no effect was observed by exposing mixed control and E/R$^+$ Ba/F3 to IL6/IL1β/TNFα in the absence of BM-MSC (27%±12% E/R$^+$, *p=ns*) (**Fig. 1**). Since it has been demonstrated that lipopolysaccharide (LPS) promotes E/R-driven leukemogenesis *in vivo* (19), we tested the effects of LPS stimulation on our competitive mesenchymal niche model but, in this case, we did not detect an advantaging effect for pre-leukemic cells (**Supplementary Fig. 2**).

Soluble factors mediated the pre-leukemia advantaging effect within the competitive inflamed niche

We then investigated if soluble factors rather than cell-cell contacts mediated the pre-leukemia-advantaging effect within the competitive mesenchymal niche in the

presence of IL6/IL1β/TNFα. As shown in **Supplementary Fig. 3A**, no differences emerged by performing experiments on 0.4µm Transwell® or direct co-cultures, indicating that secreted factors were likely the main responsible for the observation. However, we could rule out a major involvement of TGFβ because its concentration in murine BM-MSC supernatants decreased after IL6/IL1β/TNFα stimulation at all time-points considered (**Supplementary Fig. 3B**). We thus questioned about other mechanisms potentially involved. Preliminary studies on human BM-MSC cells indicated that IL6/TNFα/IL1β stimulation profoundly altered their secretory profile *in vitro* (**Supplementary Table 1**). Of note, hBM-MSC grown for 24h in the presence of the inflammatory cytokines increased secretion of chemokines binding to CXCR1 and CXCR2 receptors (CXCL1/2/3, CXCL5, CXCL6 and CXCL8); in particular, CXCL1 was the most upregulated one (**Fig. 2A**). Accordingly, murine BM-MSC dramatically increased CXCL1 release after 24h stimulation with IL6/TNFα/IL1β (inflamed: 30162±4760; unstimulated: 78±28 pg/mL; $p<0.01$), indicating conservation of the pathway across the two species (**Fig. 2B**). On the other hand, by performing gene expression profile (**Supplementary Fig. 4A**) and gene ontology analysis (**Supplementary Fig. 4B**) on E/R^+ and control Ba/F3 cells, we found that E/R^+ Ba/F3 upregulated pathways involved in the immune and inflammatory response (i.e. *inflammatory response*; *regulation of immune system process; leukocyte activation involved in the immune response*), including myeloid response (i.e. *neutrophil degranulation; myeloid cell activation involved in the immune response*). Very interesting, Ingenuity Pathway Analysis indicated that CXCR2 signaling was one of the top canonical pathways upregolated in pre-leukemic cells (**Supplementary Fig. 4C**).

Prompted by these preliminary observations, we asked if CXCR2 could play a role in the emergence of pre-leukemic cells within the competitive mesenchymal niche in the context of inflammation. To address this, we performed the competitive mesenchymal

niche assay in presence or absence of IL6/TNFα/IL1β and the specific CXCR2 inhibitor SB265610. As shown in **Supplementary Fig. 5,** inhibition of CXCR2 did not abolished the relative increase in pre-leukemic cells percentage within the inflamed niche. Similarly, addition of recombinant CXCL1 did not advantage E/R^+ cells within the competitive culture (**Supplementary Fig. 6**).

Inflamed BM-MSC preferentially attract E/R^+ pro-B cells through the CXCR2 receptor

We thus questioned about the functional significance of CXCR2 signaling activation in E/R^+ Ba/F3 cells. CXCR2 is a chemokine receptor expressed by neutrophils, macrophages, and endothelial cells that guides cells toward sites of inflammation (40,41). Recently, it has been demonstrated that CXCR2 represents a selective migratory pathway in BCP-ALL, as leukemic cells stimulate BM-MSC to secrete CXCR2 ligands which in turn attracted blasts but not normal progenitors[36]. Since we previously found that E/R expression profound impacts cell migration (26), we asked if CXCR2 signaling could have a migratory role also in E/R^+ pre-leukemic cells.

Firstly, we analyzed CXCR2 expression in control and E/R^+ Ba/F3 cells by RT-qPCR and flow-cytometry. As shown in **Fig.3A,** pre-leukemic cells strongly expressed CXCR2 at both the mRNA and surface protein levels. In contrast, control cells showed low transcriptional levels of the receptor and were negative for its membrane expression (mRNA fold increase = 140.2±45.2, $p<0.001$; MFI: E/R^+ = 1378±807; ctr = 284±167, $p<0.05$). Interestingly, E/R^+ BCP-ALL primary blasts expressed much higher levels of CXCR2 mRNA than their E/R^- counterparts, suggesting that a functional significance of the receptor could be maintained along the natural history of the disease. On the contrary, expression of CXCR1, the cognate receptor of CXCR2 (42,43), was not significantly affected in leukemic blasts of E/R^+ patients (**Supplementary Fig.7**). Although a significant

increase in CXCR1 transcription occurred in E/R$^+$ Ba/F3 cells (CXCR1 mRNA fold increase = 55.3±7.9, *p<0.001)*, no protein expression on surface was observed (**Fig.3B**).

In light of these evidences, we performed migration assay of pre-leukemic and control Ba/F3 cells towards conditioned media of BM-MSC stimulated or not with pro-inflammatory cytokines, in the presence or absence of the specific CXCR2 inhibitor SB265610 (**Fig. 4**). Inflamed BM-MSC supernatants increased migration of both normal and pre-leukemic Ba/F3 cells compared to unstimulated conditioned medium, although the increase was significant only in the latter case (% control migrated cell/input: MSC-CM=5.9±2.9; INFL.MSC-CM: 14.3±9.6, *p=ns*) (% E/R$^+$ migrated cell/input: MSC-CM= 4.6±3.3; INFL.MSC-CM: 30.2±9, *p<0.01*). In particular, E/R$^+$ cells migrated 2-fold more efficiently towards inflamed MSC-conditioned medium compared to controls (% migrated cell/input toward INFL.MSC-CM: E/R$^+$ =30.2±9.1; ctr=14.3±9.6, *p<0.01*). On the other hand, no significant differences were observed between control and E/R$^+$ Ba/F3 in case of unstimulated BM-MSC conditioned medium (% migrated cell/input toward MSC-CM: E/R$^+$=4.6±3.3; ctr=5.9±2.9, *p=ns*). As expected, CXCR2 inhibition hampered E/R$^+$ Ba/F3 cell migration, albeit to different extents: the inhibitory effect was mild and not statistically significant if cells were exposed to unstimulated conditioned-medium (%E/R$^+$ migrated cells/input: -SB265610=4.6±3.3; +SB265610=2.2±1.3, *p=ns*), whereas it was consistent and significant if exposed to inflamed supernatants (% E/R$^+$ migrated cells/input: -SB265610=30.2±9; +SB265610=7.7±4.3; *p<0.01*). In contrast, CXCR2 inhibition did not affect the migration of control cells. Altogether, these data indicate that the CXCR2 pathway mediates migration of E/R$^+$ Ba/F3 cells towards the inflamed sustaining niche although it does not directly favor the emergence of pre-leukemic cells.

Proliferation and survival of normal, but not E/R$^+$, pro-B cells decrease in the presence of BM-MSC and IL6/TNFα/IL1β

In order to better elucidate mechanisms underlying the emergence of pre-leukemic cells within the competitive inflamed niche, we analyzed proliferation and apoptosis in control and E/R$^+$ Ba/F3 cells when exposed to such microenvironmental condition (**Fig. 5A**). Consistent with our previous report (21), E/R$^+$ Ba/F3 cells cultured in standard liquid culture displayed a lower proliferative rate than control cells, as judged by higher CFSE intensity. Of note, comparable results were observed by co-culturing the Ba/F3 mix on unstimulated BM-MSC. Interestingly, both Ba/F3 cell populations cultivated on BM-MSC in the presence of IL6/IL1β/TNFα decreased proliferation compared to the unstimulated condition. However, decrease was more evident in control (CFSE MFI fold change +MSC+INFL.CK *vs* +MSC: ctr=4.4±1.8, *p<0.05*) than pre-leukemic Ba/F3 cells (CFSE MFI fold change +MSC+INFL.CK *vs* +MSC: E/R$^+$=2.2±0.6, *p<0.001*). Importantly, a striking difference was observed in terms of apoptosis: cell death, in fact, was strongly induced in control cells within the competitive inflamed niche (% ANN-V negative cells: +MSC=68.4±5.7; +MSC+INFL.CK=48.2±1.3, *p<0.05*), whereas survival of E/R$^+$ cells was completely unaffected (**Fig. 5B**).

Human normal, but not E/R$^+$, CD34$^+$IL7R$^+$ progenitors decrease in number in the presence of BM-MSC and IL6/TNFα/IL1β

Although inducible E/R-expressing Ba/F3 cells proved to be a reliable system to study E/R$^+$ pre-leukemia (21,26,38,39), we wanted to test the effects of BM-MSC and IL6/IL1β/TNFα also in a human pre-leukemic cellular model. It has been recently demonstrated that fetal CD34$^+$CD19$^-$IL7R$^+$ progenitors are the *bona fide* initiating population of E/R pre-leukemia during development (44). Thus, we asked if pre-leukemic CD34$^+$CD19$^-$IL7R$^+$ cells could be advantaged by the presence of BM-MSC and inflammation compared to controls. For this purpose, we transduced umbilical cord blood-CD34$^+$ (UCB-CD34+) progenitors with pRRL-GFP or pRRL-E/R-GFP lentiviral vectors

(control or (E/R$^+$ UCB-CD34$^+$, respectively) and separately cultured them on human BM-MSC for 72h in the presence or absence of IL6/IL1β/TNFα. By adopting this short-term culture system, the whole population lacked CD19 expression; on the contrary, a CD34$^+$IL7R$^+$ subpopulation clearly emerge in both control and pre-leukemic cells (**Supplementary Fig.8A,** *gate P7*). As experimental read-out, the relative number and percentage of total GFP$^+$ cells, CD34$^+$IL7R$^+$, CD34$^+$IL7R$^-$ and CD34$^-$ fractions was calculated for each condition (control cells+MSC; control cells+MSC+IL6/IL1β/TNFα; E/R$^+$ cells +MSC; E/R$^+$ cells +MSC+IL6/IL1β/TNFα). In case of control cells, addition of pro-inflammatory cytokines to the co-culture (**Fig. 6A**, *lower graph*) increased the number of total GFP$^+$ (tot control GFP$^+$: +MSC = 6117±1646; +MSC+INFL.CK= 8077±1087; *p<0.05*). Such increase was accompanied by the expansion of more differentiating CD34$^-$ cells and a significant reduction of CD34$^+$IL7R$^+$ progenitors (control CD34$^-$: +MSC = 3649±963; MSC+INFL.CK: 5516±622, *p<0.05*; control CD34$^+$IL7R$^+$ number: +MSC = 373±101; +MSC+INFL.CK: 254±56, *p<0.05*; control CD34$^+$IL7R$^+$ percentage: +MSC = 6.1%±0.5%; +MSC+INFL.CK: 3.1%±0.3%, *p<0.01*), while no alterations were observed in the CD34$^+$IL7R$^-$ fraction.

Regarding E/R-transduced UCB-CD34$^+$ cells, it is notable that expression of the E/R itself led to the specific expansion of the CD34$^+$IL7R$^+$ compartment, in line with previous findings (44) (**Fig. 6B,** *upper graph*; control CD34$^+$IL7R$^+$= 373±101; E/R$^+$ CD34$^+$IL7R$^+$= 635±44, *p<0.05*). On the contrary, the fusion gene had no significant impact on the CD34$^+$IL7R$^-$ and CD34$^-$ fractions in basal (non-inflamed) condition. Very interesting, in the presence of BM-MSC and inflammatory cytokines E/R-expressing CD34$^+$IL7R$^+$ progenitors were preserved from reduction, in sharp contrast to what observed in controls (E/R$^+$ CD34$^+$IL7R$^+$: +MSC = 635±44; +MSC+INFL.CK: 727±142, *p=ns*) (**Fig. 6B,** *lower graph*). On the other hand, the number of total pre-leukemic GFP$^+$ cells decreased (tot E/R$^+$ GFP$^+$: +MSC+INFL.CK= 6374±997; +MSC = 6727±1300; *p<0.05*), possibly due to a

reduction of the $CD34^-$ fraction (E/R^+ $CD34^-$: +MSC = 4403±726; +MSC+INFL.CK: 3615±542, *p<0.05*) while that of $CD34^+IL7R^-$ cells were unaffected.

Since a $CD34^{high}IL7R^+$ phenotype was recognizable in both control and E/R^+ UCB-$CD34^+$-derived populations (**Supplementary Fig. 8A,** *gate P8*), we decided to extend the analysis to this fraction as well. Similar to what observed in the general $CD34^+IL7R^+$ compartment, the $CD34^{high}IL7R^+$ fraction was significantly decreased in the control population within the inflamed BM-MSC co-culture (fold-change control +MSC+INFL.CK *vs* +MSC = 0.63±0.07; *p<0.05*), while it was slightly increased in the pre-leukemic one (fold-change E/R^+ +MSC+INFL.CK *vs* +MSC =1.09±0.03; *p<0.05*, **Supplementary Fig. 8B**).

The inflamed mesenchymal niche represents a genotoxic microenvironment for hematopoietic progenitors

Since it has been demonstrated that mesenchymal inflammation induces genotoxic stress in HSPC (37), we sought to determine the extent of DSB in control and E/R^+ Ba/F3 cells within the inflamed niche. As judged by the levels of histone 2AX phosphorylation (γH2AX), pre-leukemic cells grown under basal conditions were characterized by higher levels of DNA DSB compared to control cells (γH2AX MFI fold increase: E/R^+ = 1.86±0.65, *p<0.05*), confirming the intrinsic genotoxic activity of E/R (11) (**Fig.7A**). Interestingly, while exposure to unstimulated BM-MSCs did not affect basal γH2AX in both E/R^+ Ba/F3 and control cells, co-culturing them on BM-MSC in the presence of IL6, TNFα and IL1β increased γH2AX in both groups (γH2AX MFI fold increase +MSC+INFL.CK *vs* +MSC: E/R^+ = 2.28±1.56, *p<0.05*; ctr = 4.36±1.61, *p<0.01*). Additionally, we asked whether deregulation of activation-induced cytidine deaminase (AID), a well-established mutagenic mechanism of E/R^+ pre-leukemia to leukemia transition *in vivo* (19), may also be present in

our system. As shown in **Fig. 7B**, pre-leukemic Ba/F3 cells basally expressed higher levels of AID mRNA compared to controls (AID mRNA fold increase: E/R$^+$ *vs* ctr = 4.9±2.1, *p<0.05*). Very interesting, AID expression further increased in both control and E/R$^+$ Ba/F3 cells once exposed to the inflamed niche secretome (AID mRNA fold increase +MSC+infl.ck *vs* basal: ctr = 14.7±10.9, *p<0.05;* E/R$^+$ = 6.3±1.6). Overall, these data demonstrated that the inflamed niche represents a genotoxic microenvironment for hematopoietic progenitors that could promote malignant transformation in the apoptosis-resistant E/R$^+$ clone.

Discussion

Dysregulated inflammatory and immune responses to common infections are emerging as the main candidate risk factors for pre-leukemia to leukemia transition in BCP-ALL (45). Epidemiological studies taking into account seasonal infection peaks, time-space clustering of BCP-ALL cases and population mixing, came to the conclusion that the increase in leukemia incidence strongly correlates with infective events (16–18,45). Notably, infections and inflammation profoundly modifies the BM cellular and molecular composition by inducing a switch from the physiological hematopoiesis to a demand-adapted hematopoietic response (46). Paradoxically, many of the mechanisms that regulate HSPC during the so-called “emergency hematopoiesis”, including cytokines, growth factors, chemokines and adhesion molecules, may regulate leukemic progenitors (47), thus suggesting a possible molecular explanation for the correlation between ALL onset and infective events.

In line with this hypothesis, we and others have proposed a model in which E/R$^+$ pre-leukemic progenitors, which is known to contribute to hematopoiesis but fail to out-compete normal HSPC (10), could gain a selective advantage from the infection-induced

modifications in the BM, particularly from alterations of the local cytokine milieu (21,44). In this regard, we previously demonstrated that TGFβ, a key immune modulator produced during inflammation (48), reduces proliferation in control but not in E/R$^+$ Ba/F3 cells (21). Additionally, in this cellular model, E/R$^+$ impaired ERK phosphorilation and consequent chemotaxis in response to CXCL12 (26), a crucial cytokine for HSPC organization and functions in the niche (32,33,49). On the other hand, Torrano and colleagues showed that E/R$^+$ murine and human cells ectopically expressed the erythropoietin receptor (EPOR) and EPOR signalling mediated cell survival through the JAK2/STAT5/BCL-XL pathway activation (50). More recently, in a model of human E/R-expressing iPS that resembles the fetal B cell development, Böiers et al. have shown that pre-leukemic progenitors are characterized by a lympho-myelo gene expression profile and are able to survive in the presence of myeloid cytokines, contrarily to normal fetal progenitors (44).

Collectively, these observations indicate that E/R impacts on several pathways regulating the homeostasis of hematopoietic cells within the BM niche. On the other hand, the BM microenvironment may exert a complementary role in E/R-driven leukemogenesis. Interestingly, during infections and inflammation, BM stromal cells are able to stimulate proliferation and maturation of myeloid progenitors through the secretion of myeloid growth factors (46,47,51).

Here, we demonstrated that BM-MSC cooperate with IL6, TNFα and IL1β pro-inflammatory cytokines in favoring the persistence and potential transformation of E/R$^+$ pre-leukemic HSPC, in particular by affecting their proliferation, migration and survival, as well as DNA damage and AID expression levels. IL6, TNFα and IL1β are pleiotropic cytokines precociously secreted by pathogen receptors (PRRs)-expressing cells in response to several types of infections (52). In addition to regulate proliferation and differentiation of normal HSPC under infective conditions (47), IL6, TNFα and IL1β can

contribute to the establishment and maintenance of the leukemic niche (53–55). However, by performing competitive growth assay in the absence of BM-MSC, no advantaging effect of IL6/IL1β/TNFα on E/R-expressing pro-B cells was observed. On the other hand, E/R$^+$ Ba/F3 were not favored in the presence of unstimulated BM-MSC, indicating that the emergence of pre-leukemic cells strictly depends on IL6/IL1β/TNFα-mediated mesenchymal inflammation. Unexpectedly, no increase in E/R$^+$ Ba/F3 was observed by adding LPS to the competitive mesenchymal niche despite its role in leukemogenesis in mice (19). A possible explanation is that LPS may affect other niche component *in vivo* or may indirectly act on BM-MSC by stimulating antigen-presenting cells to secrete IL6, IL1β and TNFα. By transwell experiments, we have evidences that soluble molecules are the main determinants of the pre-leukemia sustaining effect provided by the inflamed niche. However, neither TGFβ nor CXCL1, a new candidate factor emerging from our investigations, appears to be directly involved. On this regard, it is tempting to speculate that myeloid features of E/R$^+$ Ba/F3 cells could, at least in part, account for their advantage within the inflamed niche (37,46,47,51). Interestingly, aberrant expression of myeloid genes and surface antigens is frequently observed in E/R$^+$ blasts (56) and a myelo-lympho phenotype was identified in human E/R$^+$ CD34$^+$IL7R$^+$ progenitors, a recently proposed cellular target of E/R activity during fetal hematopoiesis (44). Remarkably, we found that normal CD34$^+$IL7R$^+$ progenitors (including the CD34^{high}IL7R$^+$ fraction) are negatively affected by mesenchymal inflammation, while E/R expression specifically preserved this compartment, possibly leading to its emergence under infective/inflammatory events.

In addition to favoring pre-leukemia emergence, we found that the inflamed niche represents an attractive and genotoxic microenvironment for pre-leukemic cells. BM-MSC, in fact, strongly increased secretion of CXCR1/2 ligands after stimulation with IL6/IL1β/TNFα while pre-leukemic (but not control) Ba/F3 cells expressed the CXCR2 chemokine receptor. Accordingly, we observed robust CXCR2-dependent migration of

E/R$^+$ Ba/F3 cells towards inflamed BM-MSC supernatants. Of note, CXCR2 was overexpressed also in E/R-positive compared to E/R-negative primary blasts, suggesting a possible conserved mechanism across the natural history of the disease and clarifying the functional meaning of the CXCR2-CXCL1 axis in our model.

On the other hand, exposure to the inflamed niche increased the extent of DSB in both control and E/R$^+$ pro-B cells. However, while normal pro-B cells underwent apoptosis, E/R$^+$ Ba/F3 cells were able to persist despite accumulating genetic damages. Intriguingly, pre-leukemic Ba/F3 cells showed higher basal levels of γH2AX, indicating that, besides inducing genetic stress, E/R could trigger anti-apoptotic pathways that counteract it. In good agreement with this hypothesis, E/R has been shown to induce intracellular reactive oxygen species (ROS) in B cells (11), while affecting genes involved in the DNA damage repair (DDR) system (38,57), in particular by impairing the p53 pathway (58). In addition to DSB, E/R$^+$ Ba/F3 cells show higher basal levels of AID mRNA compared to control. Noteworthy, the genotoxic inflamed niche induces a further upregulation of AID in both cell groups. It has been demonstrated that repetitive LPS stimulation promoted E/R$^+$ pre-BII malignant transformation *in vivo* through coordinate AID and RAG activities (19). Although we could not detect expression of RAG enzymes in Ba/F3 cells (data not shown), which was expected given their developmental stage (59), a functional role for AID in these cells has been proposed (60). In a transgenic mouse model of proB ALL predisposition, AID deletion surprisingly accelerated leukemia development, while the rare proB tumors developed by AID-expressing mice showed a significant upregulation of the enzyme (60). Thus, it is tempting to speculate that increased AID levels could promote off-target mutations in the apoptosis-resistant pre-leukemic clone, contributing to its malignant transformation.

In conclusion, we propose a model where the concerted action of inflammation and BM-MSC preferentially attracts E/R$^+$ cells to a sustaining niche that negatively affects

proliferation and survival of normal hematopoietic progenitors while minimally or not impact on pre-leukemic cells, thereby providing these latter with a selective advantage over their normal counterparts. In addition, the inflamed niche predisposes pre-leukemic cells to malignant transformation by the accumulation of DNA damage and increased expression of AID enzyme. Further characterization of the crucial pathways sustaining E/R^+ pre-leukemic cells within the inflamed niche could provide mechanistic insights into E/R-driven pathogenesis. This knowledge could in turn be useful for the design of specific inhibitors that could prevent pre-leukemia to leukemia transition and avoid relapses derived from secondary evolution of pre-leukemic clones.

Acknowledgements

The authors thank Dr.Caserta Carolina for experimental support. This study was supported by grants from: Fondazione Tettamanti, Fondazione Cariplo (2018-0339), Associazione Italiana Ricerca sul Cancro (AIRC, project number IG 2018 Id. 21999, to G.C. and IG 2014 Id.15494, to G.D'A.), Beat Leukemia Foundation (www.beat-leukemia.org). L.B. was supported by scholarships from Bianchi Industrial and Società Italiana Ematologia Sperimentale (SIES). The work in PM and CB laboratory has been funded by the European Research Council (CoG-2014-646903 and PoC-2018-811220), the Agencia Estatal de Investigación/European Regional Development Fund (SAF2016-80481-R and SAF2016-75442-R) and the Catalunya Government (SGR330 and PERIS 2017) to P.M as well as the Asociación Española Contra el Cáncer, Beca FERO and the ISCIII/FEDER (PI17/01028) to C.B. P.M also acknowledges the institutional support from the Obra Social La Caixa-Fundaciò Josep Carreras.

Conflict of Interest

The authors declare no competing financial interests.

References

1. Golub TR, Barker GF, Bohlander SK, Hiebert SW, Ward DC, Bray-Ward P, *et al*. Fusion of the TEL gene on 12p13 to the AML1 gene on 21q22 in acute lymphoblastic leukemia. *Proc Natl Acad Sci*. 1995;92(11):4917–21.
2. Romana SP, Mauchauffe M, Coniat M Le, Pastier D Le, Berger R, Bernard OA. The t(12;21) of acute lymphoblastic leukemia results in a TEL-AML1 gene fusion. *Blood*. 1995;85(12):3662–70.
3. Inaba H, Greaves M, Mullighan CG. Acute lymphoblastic leukaemia. *Lancet*. 2013;381(9881):1943–55.
4. Mullighan CG. Genomic characterization of childhood acute lymphoblastic leukemia. *Semin Hematol*. 2013;50(4):314–24.
5. Ford AM, Bennett CA, Price CM, Bruin MC, Van Wering ER, Greaves M. Fetal origins of the TEL-AML1 fusion gene in identical twins with leukemia*. Proc Natl Acad Sci.* 1998;95(8):4584–8.
6. Wiemels JL, Cazzaniga G, Daniotti M, Eden OB, Addison GM, Masera G, *et al*. Prenatal origin of acute lymphoblastic leukaemia in children. *Lancet*. 1999;354:1499–503.
7. Schäfer D, Olsen M, Lähnemann D, Stanulla M, Slany R, Schmiegelow K, *et al*. Five percent of healthy newborns have an ETV6-RUNX1 fusion as revealed by DNA-based GIPFEL screening. *Blood*. 2018. p. 15:821-826.
8. Hong D, Gupta R, Ancliff P, Atzberger A, Brown J, Soneji S, *et al.* Initiating and cancer-propagating cells in TEL-AML1-associated childhood leukemia. *Science*. 2008;319(5861):336–9.
9. Tsuzuki S, Seto M, Greaves M, Enver T. Modeling first-hit functions of the t(12;21) TEL-AML1 translocation in mice. *Proc Natl Acad Sci*. 2004;101(22):8443–8.
10. Schindler JW, Van Buren D, Foudi A, Krejci O, Qin J, Orkin SH, *et al.* TEL-AML1 Corrupts Hematopoietic Stem Cells to Persist in the Bone Marrow and Initiate Leukemia. *Cell Stem Cell*. 2009;5(1):43–53.
11. Kantner H-P, Warsch W, Delogu A, Bauer E, Esterbauer H, Casanova E, *et al.* ETV6/RUNX1 Induces Reactive Oxygen Species and Drives the Accumulation of DNA Damage in B Cells. *Neoplasia*. 2013;15(11):1292-1300.
12. Levasseur M, Maung ZT, Jackson GH, Kernahan J, Proctor SJ, Middleton PG. Relapse of acute lymphoblastic leukaemia 14 years after presentation: Use of molecular techniques to confirm true re-emergence. *Br J Haematol*. 1994;87:437-8.

13. Ford AM, Fasching K, Panzer-Grümayer ER, Koenig M, Haas OA, Greaves MF. Origins of “late” relapse in childhood acute lymphoblastic leukemia with TEL-AML1 fusion genes. *Blood*. 2001;98(3):558–64.
14. Konrad M, Metzler M, Panzer S, O¨ streicher I, Peham M, Repp R, *et al.* Late relapses evolve from slow-responding subclones acute lymphoblastic leukemia : for the persistence evidence of a pre-leukemic clone. *Blood*. 2003:101:3635–40.
15. Kuster L, Grausenburger R, Fuka G, Kaindl U, Krapf G, Inthal A, *et al.* ETV6-RUNX1-positive relapses evolve from an ancestral clone and frequently acquire deletions of genes implicated in glucocorticoid signaling. *Blood*. 2018;117(9):2658–68.
16. Francis SS, Selvin S, Yang W, Buffler PA, Wiemels JL. Unusual space-time patterning of the Fallon, Nevada leukemia cluster: Evidence of an infectious etiology. *Chem Biol Interact*. 2012;196:102-109.
17. Heath CW, Hasterlik RJ. Leukemia among children in a suburban community. *Am J Med*. 1963;34(6):796–812
18. Cazzaniga G, Bisanti L, Randi G, Deandrea S, Bungaro S, Pregliasco F, *et al.* Possible role of pandemic AH1N1 swine flu virus in a childhood leukemia cluster. *Leukemia*. 2017;31(8):1819–21.
19. Swaminathan S, Klemm L, Park E, Papaemmanuil E, Ford A, Kweon SM, *et al.* Mechanisms of clonal evolution in childhood acute lymphoblastic leukemia. *Nat Immunol.* 2015;16(7):766–74.
20. Rodríguez-Hernández G, Hauer J, Martín-Lorenzo A, Schäfer D, Bartenhagen C, García-Ramírez I, *et al.* Infection exposure promotes ETV6-RUNX1 precursor B-cell leukemia via impaired H3K4 demethylases. *Cancer Res*. 2017;77(16):4365–77.
21. Ford AM, Palmi C, Bueno C, Hong D, Cardus P, Knight D, *et al.* The TEL-AML1 leukemai fusion gene dysregulates the TGF-beta pathway in early B lineage progenitor cells. *J Clin Invest*. 2009;119(4).
22. Papaemmanuil E, Rapado I, Li Y, Potter NE, Wedge DC, Tubio J, *et al.* RAG-mediated recombination is the predominant driver of oncogenic rearrangement in ETV6-RUNX1 acute lymphoblastic leukemia. *Nat Genet*. 2014;46(2):116–25.
23. Naderi EH, Skah S, Ugland H, Myklebost O, Sandnes DL, Torgersen ML, *et al.* Bone marrow stroma-derived PGE2 protects BCP-ALL cells from DNA damage-induced p53 accumulation and cell death. *Mol Cancer*. 2015;14(14).
24. Polak R, De Rooi B, Pieters R. B-cell precursor acute lymphoblastic leukemia cells use tunneling nanotubes to orchestrate their microenvironment. *Blood*. 2015;126(21):2404–14.

25. Forsberg EC, Smith-Berdan S. Parsing the niche code: The molecular mechanisms governing hematopoietic stem cell adhesion and differentiation. *Haematologica*. 2009;94(11):1477–81.
26. Palmi C, Fazio G, Savino AM, Procter J, Howell L, Cazzaniga V, *et al.* Cytoskeletal Regulatory Gene Expression and Migratory Properties of B-cell Progenitors Are Affected by the ETV6-RUNX1 Rearrangement. *Mol Cancer Res*. 2014;12(12):1796–806.
27. Méndez-Ferrer S, Michurina T V., Ferraro F, Mazloom AR, MacArthur BD, Lira SA, *et al.* Mesenchymal and haematopoietic stem cells form a unique bone marrow niche. *Nature*. 2010;466(7308):829–34.
28. Kfoury Y, Scadden DT. Mesenchymal cell contributions to the stem cell niche. *Cell Stem Cell*. 2015;16(3):239–53.
29. Tokoyoda K, Egawa T, Sugiyama T, Choi B Il, Nagasawa T. Cellular niches controlling B lymphocyte behavior within bone marrow during development. *Immunity*. 2004; 20(6):707-18.
30. Lo V, Ramı M, Moreno IC, Garcı J. Mesenchymal Stromal Cells Derived from the Bone Marrow of Acute Lymphoblastic Leukemia Patients Show Altered BMP4 Production: Correlations with the Course of Disease. *PLoS One*. 2014;9(1):1–11.
31. Reikvam H, Brenner AK, Hagen KM, Liseth K, Skrede S, Hatfield KJ, *et al.* The cytokine-mediated crosstalk between primary human acute myeloid cells and mesenchymal stem cells alters the local cytokine network and the global gene expression profile of the mesenchymal cells. *Stem Cell Res*. 2015;15(3):530–41.
32. Balandràn JC, Purizaca J, Enciso J, Dozal D, Sandoval A, Jiménez-Hernàndez E, *et al.* Pro-inflammatory-related loss of CXCL12 niche promotes acute lymphoblastic leukemic progression at the expense of normal lymphopoiesis. *Front Immunol*. 2017;7:1–14.
33. De Rooij B, Polak R, Van Den Berk LCJ, Stalpers F, Pieters R, Den Boer ML. Acute lymphoblastic leukemia cells create a leukemic niche without affecting the CXCR4/CXCL12 axis. *Haematologica*. 2017;102(10):e389–93.
34. Bernardo ME, Fibbe WE. Mesenchymal stromal cells: Sensors and switchers of inflammation. *Cell Stem Cell*. 2013;13(4):392–402.
35. Lilly AJ, Johnson WE, Bunce CM. The haematopoietic stem cell niche: New insights into the mechanisms regulating haematopoietic stem cell behaviour. *Stem Cells Int*. 2011.
36. Asada N. Regulation of Malignant Hematopoiesis by Bone Marrow Microenvironment. *Front Oncol*. 2018;23(8):119.
37. Zambetti NA, Ping Z, Chen S, Kenswil KJG, Mylona MA, Sanders MA, *et al.* Mesenchymal Inflammation Drives Genotoxic Stress in Hematopoietic Stem Cells and

Predicts Disease Evolution in Human Pre-leukemia. *Cell Stem Cell*. 2016; 3;19(5):613-627.

38. Linka Y, Ginzel S, Krüger M, Novosel A, Gombert M, Kremmer E, *et al.* The impact of TEL-AML1 (ETV6-RUNX1) expression in precursor B cells and implications for leukaemia using three different genome-wide screening methods. Blood Cancer *J*. 2013; 11;3:e151.
39. Diakos C, Krapf G, Gerner C, Inthal A, Lemberger C, Ban J, *et al.* RNAi-mediated silencing of TEL/AML1 reveals a heat-shock protein- and survivin-dependent mechanism for survival. *Blood. 2007*; 15;109(6):2607-10.
40. Richardson RM, Marjoram RJ, Barak LS, Snyderman R. Role of the Cytoplasmic Tails of CXCR1 and CXCR2 in Mediating Leukocyte Migration, Activation, and Regulation. *J Immunol*. 2003;170(6):2904–11.
41. Schraufstatter IU, Chung J, Burger M. IL-8 activates endothelial cell CXCR1 and CXCR2 through Rho and Rac signaling pathways. *Am J Physiol Lung Cell Mol Physiol.* 2001; 280(6):L1094-103.
42. Stillie R, Farooq SM, Gordon JR, Stadnyk AW. The functional significance behind expressing two IL-8 receptor types on PMN. *J Leukoc Biol*. 2009;86(3):529–43.
43. Rosu-Myles M, Khandaker M, Wu DM, Keeney M, Foley SR, Howson-Jan K, *et al.* Characterization of chemokine receptors expressed in primitive blood cells during human hematopoietic ontogeny. *Stem Cells*. 2000; 18(5):374-81.
44. Böiers C, Richardson SE, Laycock E, Zriwil A, Turati VA, Brown J, *et al.* A Human IPS Model Implicates Embryonic B-Myeloid Fate Restriction as Developmental Susceptibility to B Acute Lymphoblastic Leukemia-Associated ETV6-RUNX1. *Dev Cell. 2018*;44(3):362-377.e7.
45. Greaves M. A causal mechanism for childhood acute lymphoblastic leukaemia. *Nat Rev Cancer*. 2018;18(8):471–84.
46. Takizawa H, Boettcher S, Manz MG. Demand-adapted regulation of early hematopoiesis in infection and inflammation. *Blood*. 2012;119(13):2991-3002.
47. Riether C, Schürch CM, Ochsenbein AF. Regulation of hematopoietic and leukemic stem cells by the immune system. *Cell Death Differ*. 2015;22(2):187–98.
48. Vignali DAA, Collison LW, Workman CJ. How regulatory T cells work. *Nature Reviews Immunology*. 2008. 8(7):523-32.
49. Greenbaum A, Hsu YS, Day RB, Schuettpelz LG, Christopher J, Borgerding JN, *et al.* CXCL12 Production by Early Mesenchymal Progenitors is Required for Hematopoietic Stem Cell Maintenance. *Nature*. 2013;495(7440):227–30.

50. Torrano V, Procter J, Cardus P, Greaves M, Ford AM. ETV6-RUNX1 promotes survival of early B lineage progenitor cells via a dysregulated erythropoietin receptor. *Blood*. 2011;118(18):4910–8.
51. Day RB, Bhattacharya D, Nagasawa T, Link DC. Granulocyte colony-stimulating factor reprograms bone marrow stromal cells to actively suppress B lymphopoiesis in mice. *Blood*. 2018;125(20):3114–8.
52. Swiergiel AH, Dunn AJ. The roles of IL-1, IL-6, and TNFα in the feeding responses to endotoxin and influenza virus infection in mice. *Brain Behav Immun*. 1999; 13(3):252-65.
53. Vilchis-Ordoñez A, Contreras-Quiroz A, Vadillo E, Dorantes-Acosta E, Reyes-López A, Quintela-Nuñez Del Prado HM, *et al.* Bone marrow cells in acute lymphoblastic leukemia create a proinflammatory microenvironment influencing normal hematopoietic differentiation fates. *Biomed Res Int*. 2015;2015:386165.
54. Kagoya Y, Yoshimi A, Kataoka K, Nakagawa M, Kumano K, Arai S, *et al.* Positive feedback between NF-κB and TNF-α promotes leukemia-initiating cell capacity. *J Clin Invest*. 2014; 124(2):528-42.
55. Carey A, Edwards DK, Eide CA, Newell L, Traer E, Medeiros BC, *et al.* Identification of Interleukin-1 by Functional Screening as a Key Mediator of Cellular Expansion and Disease Progression in Acute Myeloid Leukemia. *Cell Rep*. 2017; 28;18(13):3204-3218.
56. Gerr H, Zimmermann M, Schrappe M, Dworzak M, Ludwig WD, Bradtke J, *et al.* Acute leukaemias of ambiguous lineage in children: Characterization, prognosis and therapy recommendations. *Br J Haematol*. 2010; 149(1):84-92.
57. Fuka G, Kauer M, Kofler R, Haas OA, Panzer-Grümayer R. The leukemia-specific fusion gene etv6/runx1 perturbs distinct key biological functions primarily by gene repression. *PLoS One*. 2011; 6(10):e26348.
58. Kaindl U, Morak M, Portsmouth C, Mecklenbräuker A, Kauer M, Zeginigg M, *et al.* Blocking ETV6/RUNX1-induced MDM2 overexpression by Nutlin-3 reactivates p53 signaling in childhood leukemia. *Leukemia*. 2014; 28(3):600-8.
59. Clark MR, Mandal M, Ochiai K, Singh H. Orchestrating B cell lymphopoiesis. *Nat Publ Gr*. 2013;14(2):69–80.
60. Auer F, Ingenhag D, Pinkert S, Kracker S, Hacein-Bey-Abina S, Cavazzana M, *et al.* Activation-induced cytidine deaminase prevents pro-B cell acute lymphoblastic leukemia by functioning as a negative regulator in Rag1 deficient pro-B cells. *Oncotarget*. 2017; 8(44):75797-75807.

Figure Legend

Fig.1: Inflammation favors the emergence of E/R$^+$ Ba/F3 cells in an model of competitive mesenchymal niche. A mixture of E/R$^+$ and control Ba/F3 cells (80%:20%) was grown under the indicated conditions. BASAL: standard liquid culture; +TGFβ: standard liquid culture + TGFβ (10ng/mL); + inflammatory cytokines (INFL. CK): standard liquid culture + IL6 (20ng/mL), TNFα (50ng/mL) and IL1β (25ng/mL); +MSC: Ba/F3 and murine BM-MSC co-culture; +MSC+INFL.CK: Ba/F3 and murine BM-MSC co-culture +IL6, TNFα and IL1β. After 4 days, the percentage of E/R$^+$ cells in the mix was quantified by flow cytometry using a FITC-conjugated anti-V5 tag antibody. An anti-mCD45 was used to discriminate between MSC (mCD45$^-$) and Ba/F3 cells (mCD45$^+$). Peak histograms in the figure are from a representative experiment, while values indicate mean±SD of 6 independent experiments. Paired Student's t-test (**, *p<0.01*) was applied to compare the percentage of E/R$^+$ cells grown for 4 days under the indicated conditions *vs* the basal culture.

Fig.2: BM-MSC increase secretion of CXCR1/2 ligands after stimulation with pro-inflammatory cytokines. A) Human BM-MSCs from three different healthy-donors were grown in 2% FBS-supplemented media in presence or absence of IL6 (40ng/mL), IL1β (50ng/mL) and TNFα (100ng/mL) for 24 h. Conditioned media (CM) were collected, centrifuged, and analyzed by Human Cytokines Array C1000 protein arrays (RayBio). Data were acquired through the UVITEC Cambridge® instrument and densitometry quantification performed by ImageJ® software. For each donor, protein fold-changes (FC) of inflamed *vs* unstimulated supernatants were calculated. The table shows the FC mean values of the 10 most upregulated proteins obtained in three independent experiments; the

indicated *p*-values were calculated by Student's t-test. CXCR1/2 ligands are indicated in grey. **B)** CXCL1 quantification by enzyme-linked immunosorbent assay (ELISA) in the supernatants of murine BM-MSCs grown in 2% FBS-supplemented media in the absence (MSC) or presence of IL6, TNFα and IL1β (MSC+INFL.CK) for 24h. Values are shown as mean±SD of 3 independent experiments. Student's t-test: **, *p<0.01*.

Fig.3: Overexpression of CXCR2 mRNA and cell surface protein in E/R$^+$ Ba/F3 cells. **A)** RT-qPCR analysis of CXCR1 and CXCR2 mRNA expression in control and E/R$^+$ Ba/F3 cells after 72 h of mifepristone treatment. cDNA was subjected to TaqMan qRT-PCR and normalized for *Hprt* gene expression. Values are shown as mean±SD of 6 independent experiments; for each experiment, the $2^{-\Delta\Delta Ct}$ value of Ba/F3 control was considered as reference. One sample t-test: §§§, *p<0.001*. **B)** CXCR1 and CXCR2 protein membrane expression was quantified as mean fluorescence intensity (MFI) by FACS analysis. In the scattered dot plot, values are expressed as mean±SD of 6 independent experiments. Student's t-test: *, *p<0.05*.

Fig.4: Enhanced migration of E/R$^+$ Ba/F3 cells towards inflamed BM-MSC conditioned medium is CXCR2-dependent. Transwell® migration (3h) of control and E/R$^+$ Ba/F3 towards basal (MSC-CM) or inflamed (INFL.MSC-CM) MSC supernatant in the presence or absence of the CXCR2-inhibitor SB265610 (1 µM). The number of migrated cells was determined by flow-cytometry. A set number of fluorescent reference beads (BD Trucount® tubes) was used as internal calibrator, as described in the Material and Methods. Cells were counted in technical triplicates for 30 seconds. The percentage of migrated cells was determined by dividing the number of cells in the lower chamber by the number of cells loaded into the upper chamber (input). Values are given as mean±SD of 5 independent experiments. Paired Student's t-test: **, *p<0.01*.

Fig.5: Differential effect of the inflamed mesenchymal niche on the proliferation and survival of ER- and ER+ Ba/F3 cells. A) E/R$^+$ and control Ba/F3 cells were stained with carboxyfluorescein succinimidyl ester (CFSE) and co-cultured (80%:20%) for 4 days in standard liquid culture (basal) or on murine BM-MSC monolayers in the presence or absence of IL6/TNFα/IL1β. CFSE MFI of mCD45$^+$ cells was evaluated by flow-cytometry. The E/R$^+$ fraction was detected thanks to a specific antibody against the E/R fusion sequence in place of the FITC-conjugated anti-V5 antibody. MFI of control Ba/F3 in basal condition at the end of the culture was considered as reference for fold increase calculation. The graph shows mean±SD of 5 independent experiments. §§§, *p<0.001*, one-sample t-test; paired Student's t-test: *, *p<0.05*; **, *p<0.01*; ***, *p<0.001*. FC: fold change **B)** E/R$^+$ and control Ba/F3 (80%:20%) were grown as above in the presence or absence of inflammatory cytokines. For each condition, the percentage of mCD45$^+$/annexin-V$^-$ cells was evaluated, and E/R+ cells quantified using the FITC-conjugated anti-V5 antibody. The graph shows mean±SD of 3 independent experiments: Paired Student's t-test: *, *p<0.05*; **, *p<0.01*.

Fig.6: ETV6/RUNX1 safeguards the number of human CD34$^+$IL7R$^+$ in the presence of BM-MSC and inflammation. Transfected control and E/R-expressing human UCB-CD34$^+$ cells were separately grown in stem culture medium on BM-MSC in the absence (+MSC) or presence of IL6/TNFα/IL1β (+MSC+INFL.CK) for 72 h. At the end of the culture, cells were stained with anti-CD34 and anti-IL7Rα antibodies and counted by FACS. The cell number was normalized to a determined number of fluorescent reference beads (BD Trucount® tubes) added into tubes and to the percentage of GFP positivity in the two groups. Percentages of CD34$^-$, CD34$^-$IL7R$^+$ and CD34$^+$IL7R$^+$ fractions in control UCB-CD34$^+$-derived population (**A**) and in E/R$^+$ UCB-CD34$^+$-derived population (**B**) after 72h of

culture at the indicated conditions. Values indicate the number of cells relatively quantified by flow-cytometry (mean±SD of one infection experiment in which cells were cultivated on three different healthy donor-derived BM-MSC). Paired Student's t-test: * = same experimental group, inflamed *vs* non-inflamed condition; $^{\#}$ = same experimental condition, control *vs* E/R^{+} group; $^{*,\#}$, *p<0.05*; $^{\#\#}$, *p<0.01*.

Fig.7: The inflamed mesenchymal niche increases DNA double strand breaks and AID expression in both control and E/R^{+} Ba/F3 cells. **A)** E/R^{+} and control Ba/F3 cells were co-cultured (80%:20%) for 4 days in standard liquid culture (basal) or on murine BM-MSC monolayers in the presence or absence of IL6/TNFα/IL1β. Phosphorylated levels of H2AX (γH2AX) in mCD45^{+}, both V5-positive and V5-negative, cells were measured as MFI by FACS. The MFI of control Ba/F3 cells grown under basal condition was considered as reference for fold increase calculation. Values are expressed as mean±SD of 6 independent experiments. One sample t-test: §, *p<0.05*. Paired Student's t-test: *, *p<0.05*; **, *p<0.01*. **B)** Control and E/R^{+} Ba/F3 cells were separately grown in standard liquid culture (basal) or loaded into the upper chamber of 0.4µm Transwell® inserts in the presence of MSC (lower chamber) and inflammatory cytokines (+MSC+INFL.CK). RT-qPCR analysis was performed to quantify AID expression, normalizing values on *Hprt* expression. Analysis was performed on 3 experimental triplicates. Paired Student's t-test: *, *p<0.05*; **, *p<0.01*.

Fig. 1

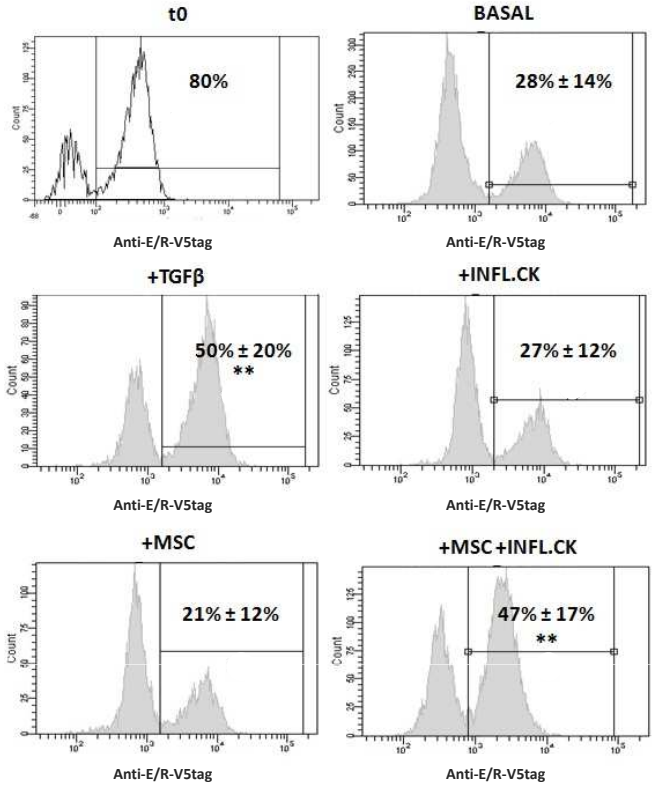
t0
80%
Anti-E/R-V5tag
BASAL
28% ± 14%
Anti-E/R-V5tag
+TGFβ
50% ± 20%
**
Anti-E/R-V5tag
+INFL.CK
27% ± 12%
Anti-E/R-V5tag
+MSC
21% ± 12%
Anti-E/R-V5tag
+MSC +INFL.CK
47% ± 17%
**
Anti-E/R-V5tag

Fig. 2

A

	FC	*p-value*
CXCL1 (GROalpha)	**304,99**	***0,018***
GRO-family	**14,30**	***0,003***
CXCL8	**12,02**	***0,001***
GM-CSF	10,33	*0,061*
betaFGF	9,32	*0,011*
CXCL6	**8,77**	***0,045***
CCL5	6,29	*0,064*
betaNGF	5,65	*0,051*
CXCL5	**4,77**	***0,007***
HGF	4,00	*0,025*

B

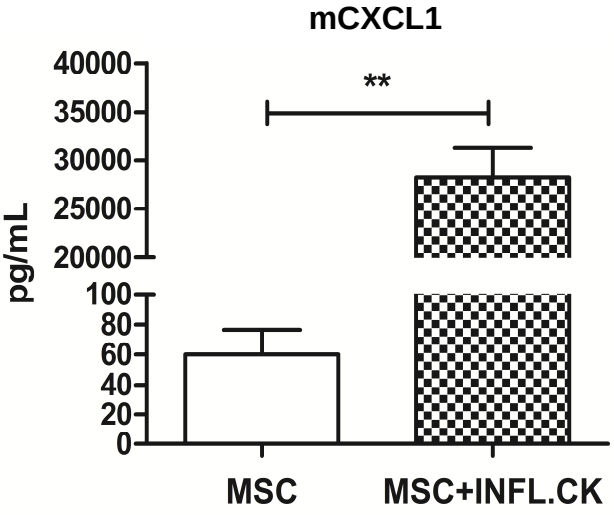

Fig. 3

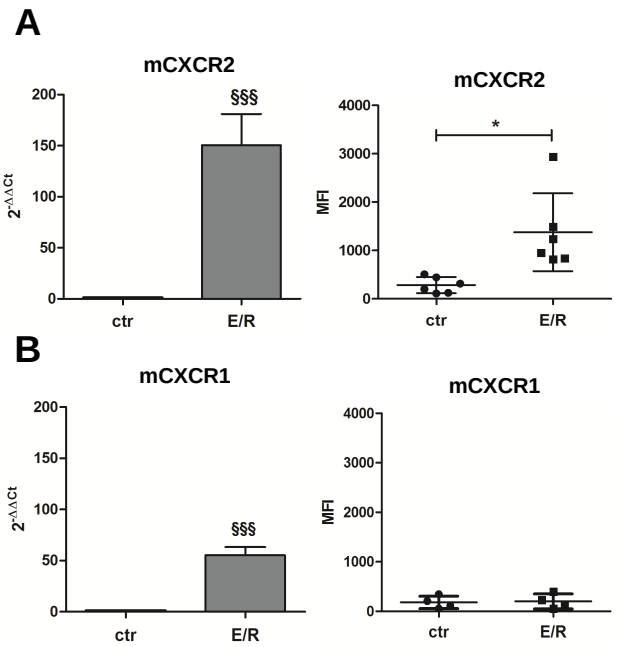
A
mCXCR2
§§§
200
150
100
50
0
2^-ΔΔCt
ctr
E/R
mCXCR2
*
4000
3000
2000
1000
0
MFI
ctr
E/R
B
mCXCR1
§§§
200
150
100
50
0
2^-ΔΔCt
ctr
E/R
mCXCR1
4000
3000
2000
1000
0
MFI
ctr
E/R

Fig. 4

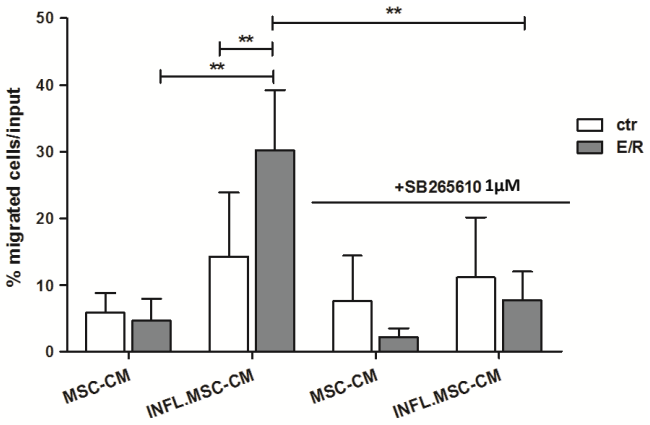
% migrated cells/input
50
40
30
20
10
0
**
**
**
ctr
E/R
+SB265610 1µM
MSC-CM
INFL.MSC-CM
MSC-CM
INFL.MSC-CM

Fig. 5

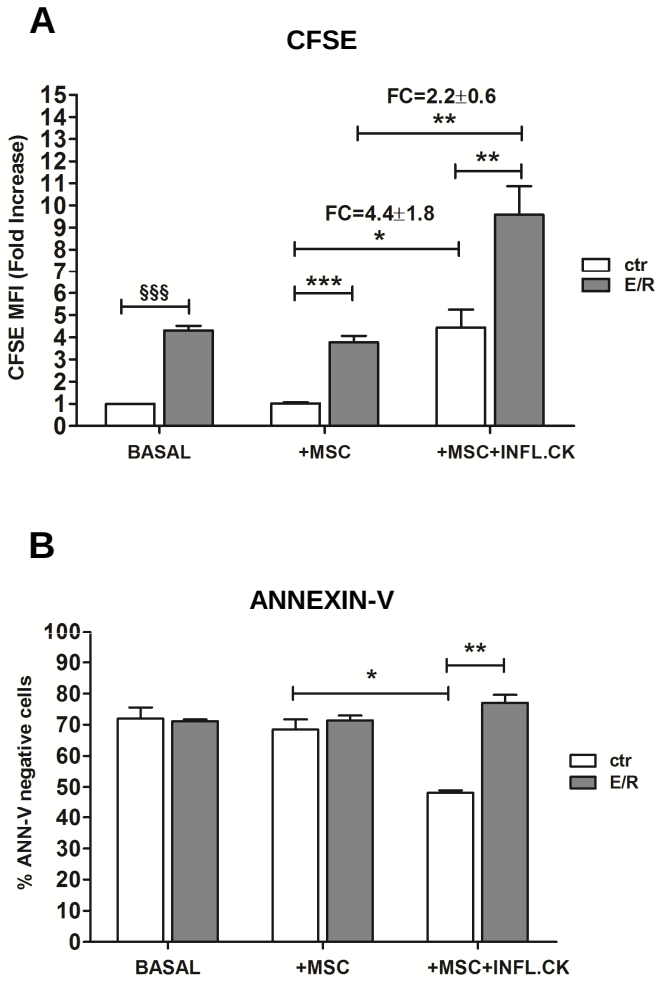
A
CFSE
CFSE MFI (Fold Increase)
FC=2.2±0.6
**
**
FC=4.4±1.8
*
***
§§§
ctr
E/R
BASAL
+MSC
+MSC+INFL.CK
B
ANNEXIN-V
% ANN-V negative cells
*
**
ctr
E/R
BASAL
+MSC
+MSC+INFL.CK

Fig. 6

A

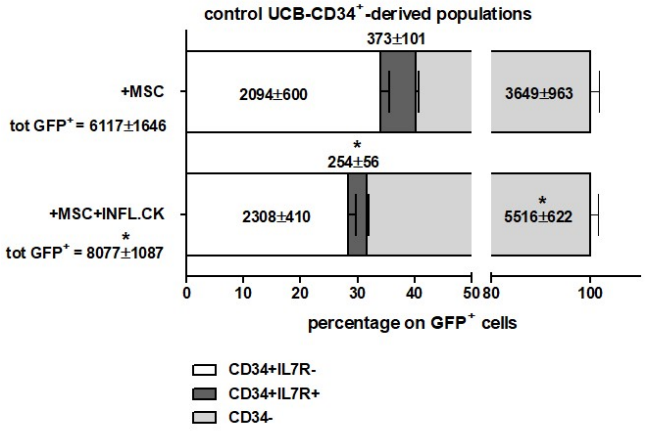
control UCB-CD34+-derived populations
373±101
+MSC
2094±600
3649±963
tot GFP+ = 6117±1646
*
254±56
+MSC+INFL.CK
2308±410
*
5516±622
*
tot GFP+ = 8077±1087
0
10
20
30
40
50
80
100
percentage on GFP+ cells
CD34+IL7R-
CD34+IL7R+
CD34-

B

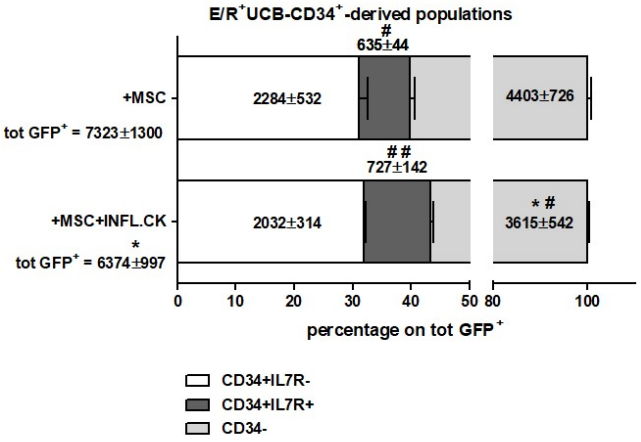
E/R+UCB-CD34+-derived populations
#
635±44
+MSC
2284±532
4403±726
tot GFP+ = 7323±1300
##
727±142
+MSC+INFL.CK
2032±314
* #
3615±542
*
tot GFP+ = 6374±997
0
10
20
30
40
50
80
100
percentage on tot GFP+
CD34+IL7R-
CD34+IL7R+
CD34-

Fig. 7

A

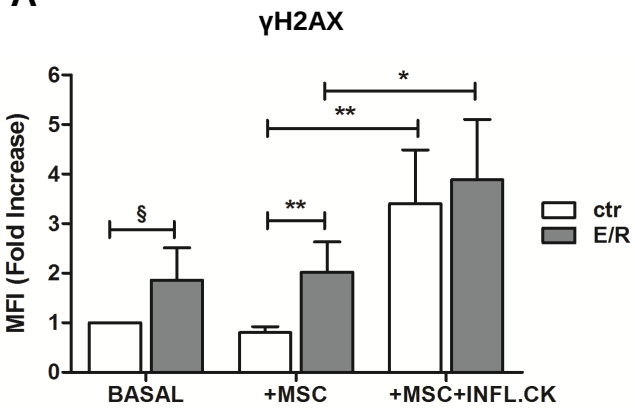
γH2AX
MFI (Fold Increase)
6
5
4
3
2
1
0
§
**
**
*
ctr
E/R
BASAL
+MSC
+MSC+INFL.CK

B

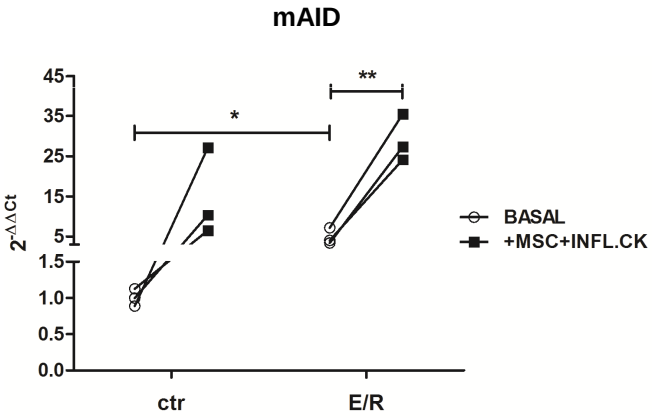
mAID
2^-ΔΔCt
45
35
25
15
5
1.5
1.0
0.5
0.0
*
**
BASAL
+MSC+INFL.CK
ctr
E/R

Supplementary Fig.1

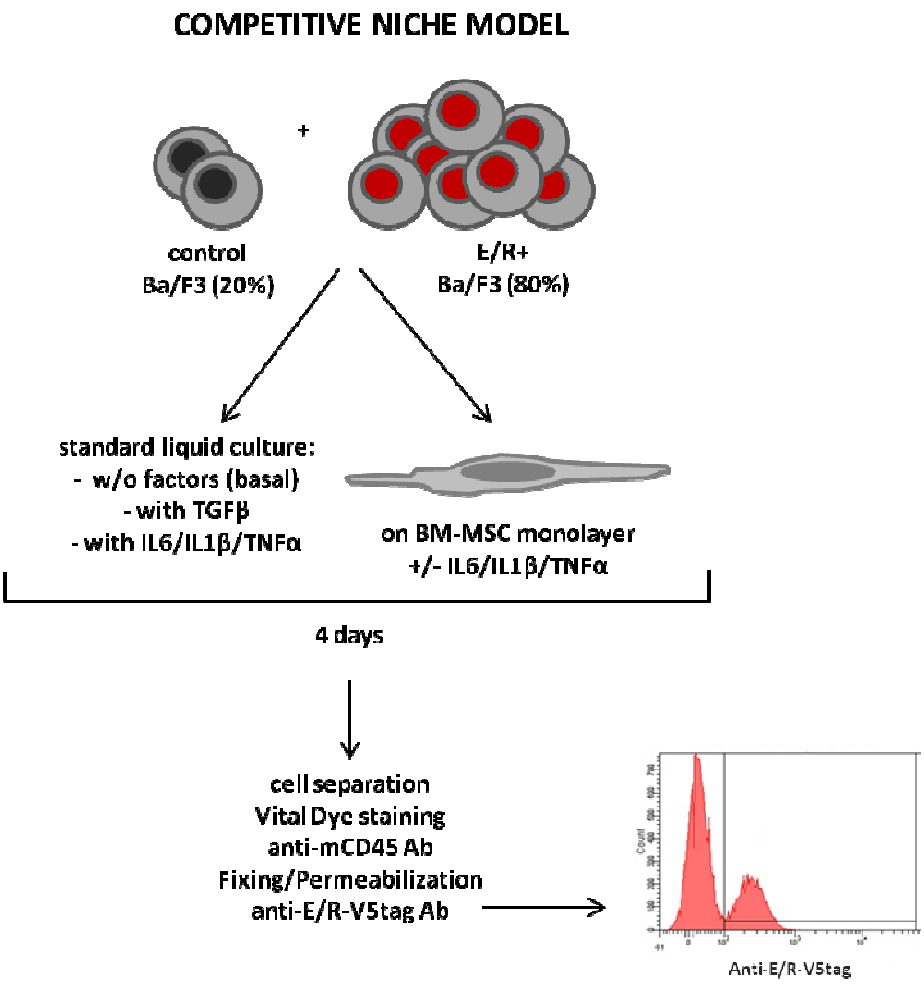

Fig.S1: Schematic representation of the competitive niche assay. Control and E/R$^+$ Ba/F3 cells were mixed at a starting ratio of 20%:80% (t0) and cultivated for 4 days on murine BM-MSC monolayers in the presence or absence of IL6 (20ng/mL), IL1β (25ng/mL) and TNFα (50ng/mL). As control, mixed Ba/F3 cells were cultured in standard liquid culture without cytokines (basal condition) and in the presence of TGFβ (10ng/mL) or IL6/IL1β/TNFα. After 4 days, cells were trypsinized and stained with Horizon^{TM} Fixable Viability Stain 450 and a PE-conjugated anti mCD45 antibody. Cells were then fixed-permeabilized and stained with the FITC-conjugated anti-V5tag antibody to distinguish E/R-expressing Ba/F3 from negative controls. Percentages of FITC$^+$ and FITC$^-$ cells were evaluated by flow-cytometry by gating on the Horizon450$^-$/mCD45$^+$ population.

Supplementary Fig.2

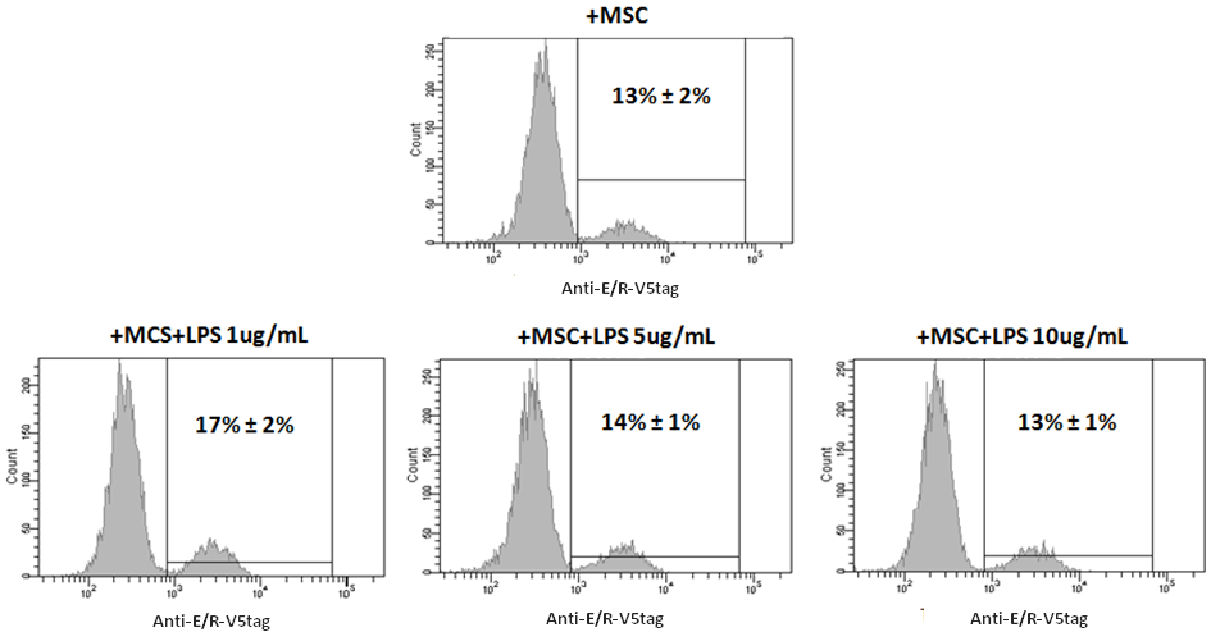

Fig.S2: LPS stimulation does not provide advantage to E/R$^+$ Ba/F3 in the competitive niche. Control and E/R$^+$ Ba/F3 cells were cultured as described in the Legend to Fig. S1 in the presence or absence of increasing doses of LPS. Peaks are from a representative experiment while values indicate mean±SD of 3 independent experiments.

Supplementary Fig.3

A

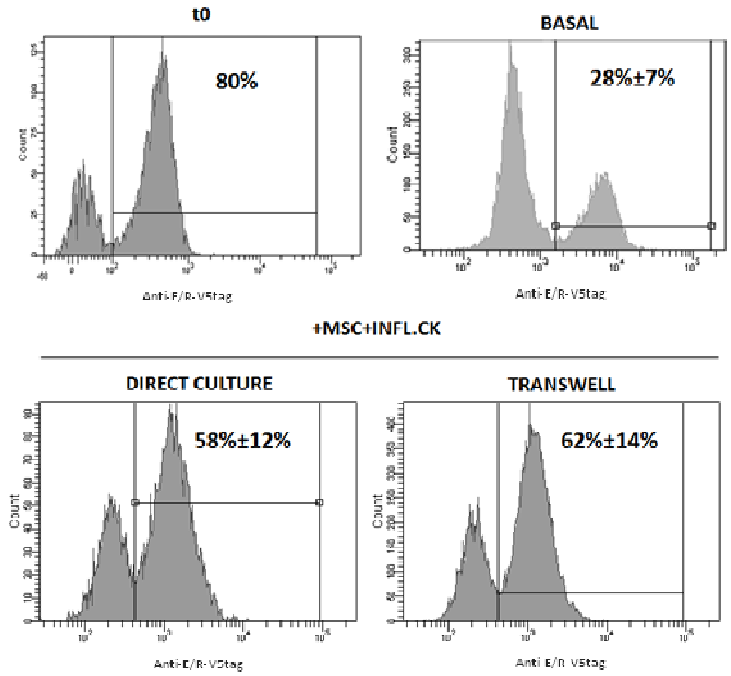

B

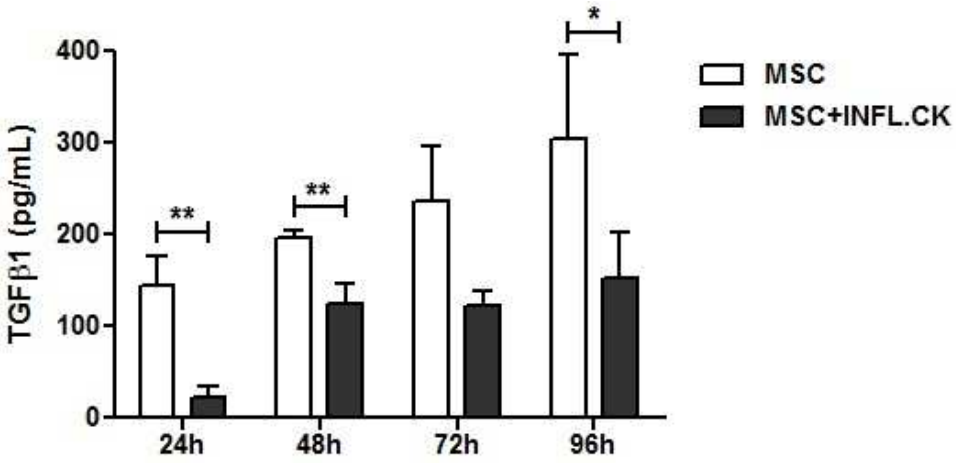

Fig.S3: Soluble factors mediate the pre-leukemia selective advantage within the inflamed competitive niche. A) Control and E/R^{+} Ba/F3 cells were cultured as described in the Legend to Fig. S1 in the presence of IL6/IL1β/TNFα either in direct contact with BM-MSC monolayers or separated by a 0.4µm Transwell® insert. Peaks are from a representative experiment while values indicating mean±SD of 3 independent experiments. **B)** ELISA quantification of TGFβ in the supernatants of murine BM-MSC

stimulated or not with IL6/IL1β/TNFα. Results are presented as mean±SD of 3 independent experiments. Paired Student's t-test: *, $p<0.05$; **, $p<0.01$.

Supplementary Fig.4

A

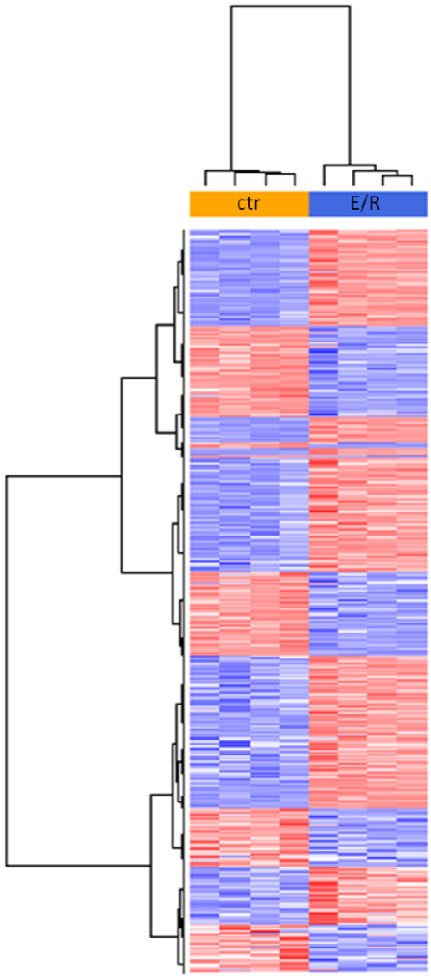

B

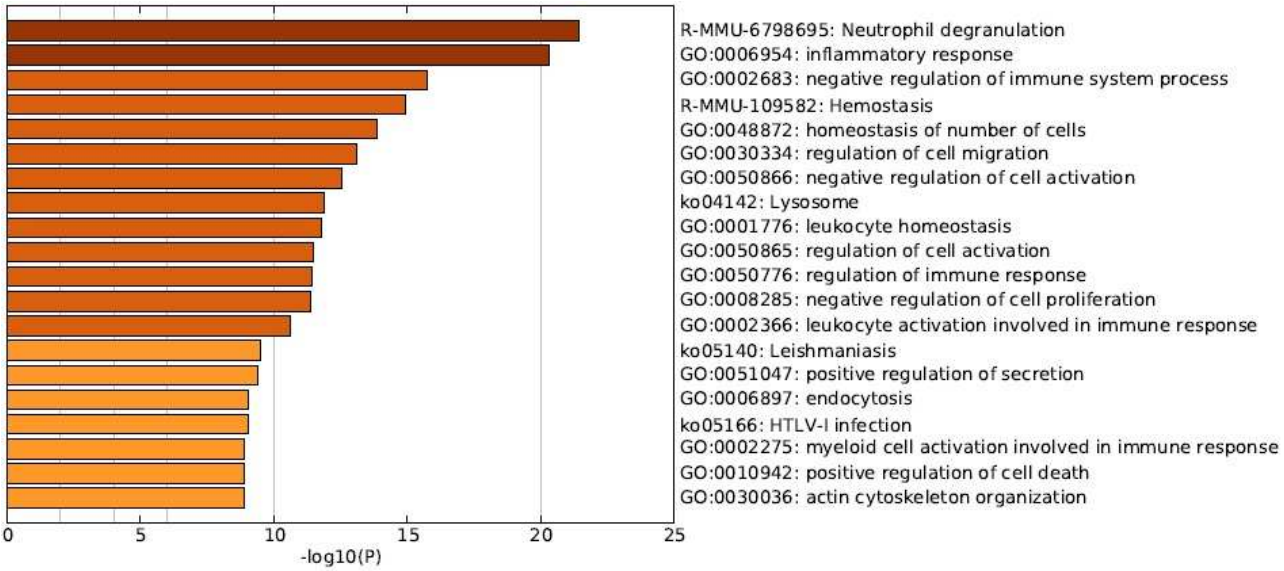

C

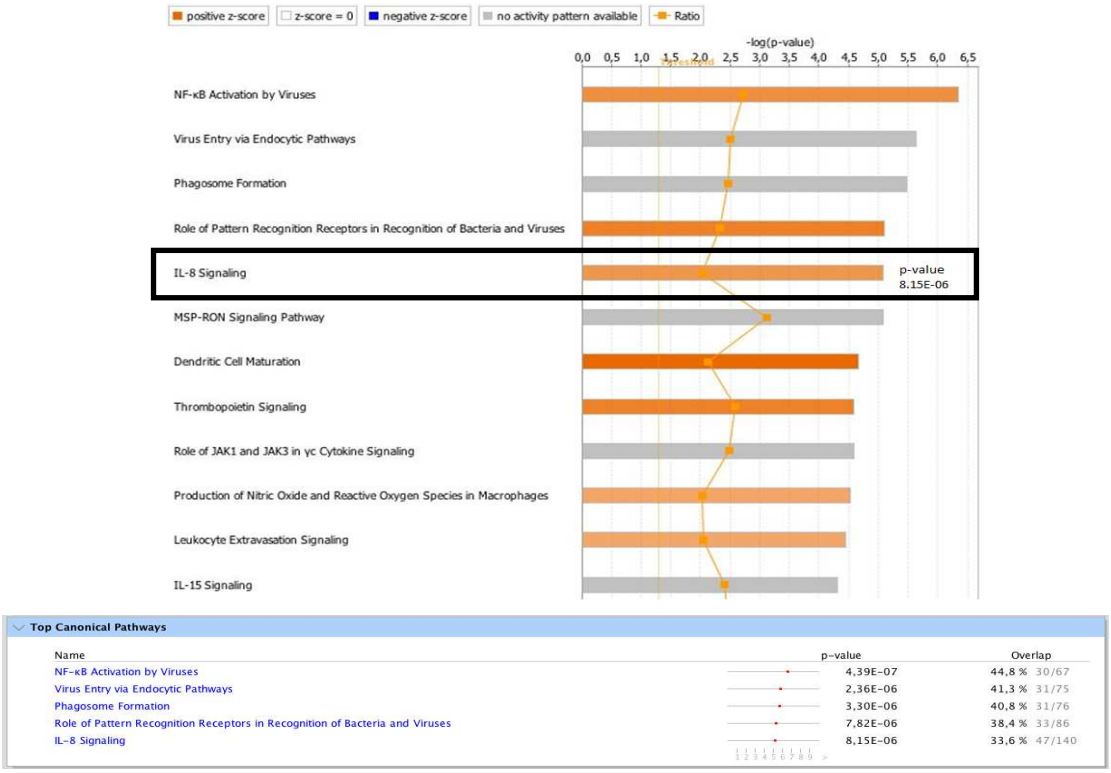

Fig.S4: A) **Gene expression profiling by Gene Chip Mouse 2.0 Arrays of control and E/R^{+} Ba/F3 cells**. Only those E/R induction experiments showing >90% viability and >90% FITC positivity were chosen for analysis (n=3). **B) E/R^{+} Ba/F3 upregulated pathways involved in the immune and inflammatory response, included myeloid response.** Gene ontology (GO) analysis was performed by Metascape. Differentially expressed genes were identified by significance analysis of microarray (SAM) algorithm coded in the samr R package and by estimating the percentage of false positive predictions (i.e. false discovery rate, FDR) with 100 permutations; *q-value<0.01*. In the dendogram, the 20 best *p*-values are indicated. **C) CXCR2 (IL-8) signaling was one of the top canonical pathways upregolated in pre-leukemic cells.** Ingenuity Pathway Analysis was performed on filtered GEP data (E/R^{+} *vs* control Ba/F3: FC < 0.75 and FC > 1.5). As evidenced, the CXCR2 (IL-8) signaling was activated in pre-leukemic Ba/F3 compared to controls.

Supplementary Fig.5

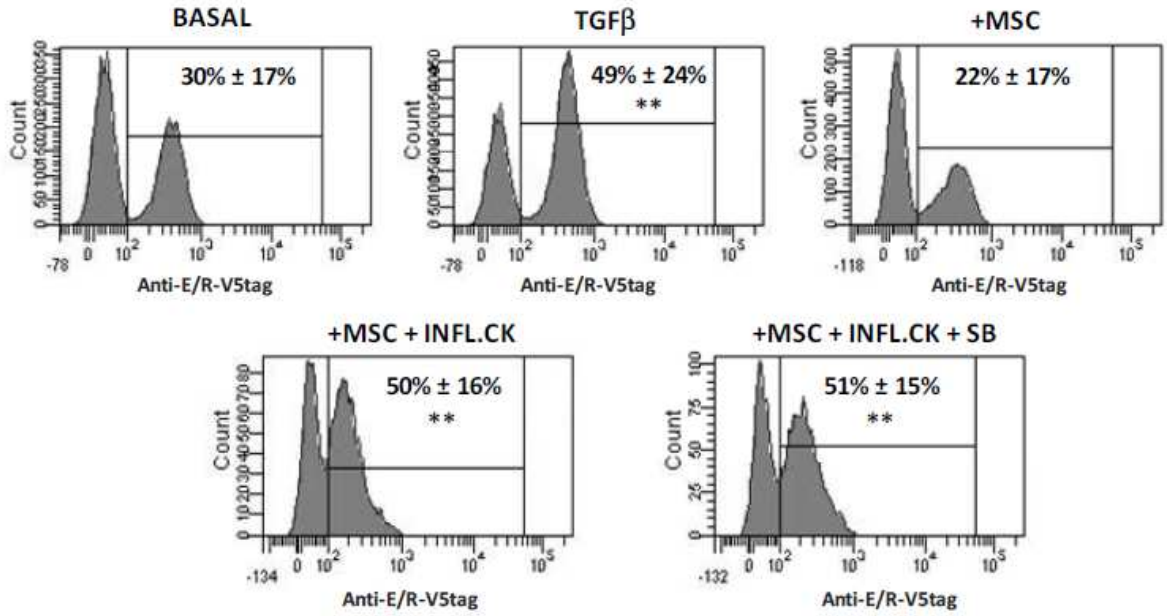

Fig.S5: Inhibition of CXCR2 did not abolished the relative increase of pre-leukemic cells percentage within the inflamed niche. A mixture of E/R$^+$ and control Ba/F3 cells (80%:20%) was grown under the indicated conditions. BASAL: standard liquid culture; +TGFβ: standard liquid culture + TGFβ (10ng/mL); +MSC: Ba/F3 and murine BM-MSC co-culture; +MSC+INFL.CK: Ba/F3 and murine BM-MSC co-culture +IL6, TNFα and IL1β; +MSC+INFL.CK+SB: Ba/F3 and murine BM-MSC co-culture +IL6, TNFα and IL1β in the presence of CXCR2 inhibitor SB265610 (1µM). After 4 days, the percentage of E/R+ cells in the mix was quantified by flow cytometry using a FITC-conjugated anti-V5 tag antibody. An anti-mCD45 was used to discriminate between MSC (mCD45-) and Ba/F3 cells (mCD45+). Peak histograms in the figure are from a representative experiment, while values indicate mean±SD of 4 independent experiments. Paired Student's t-test (*, $p<0.05$) was applied to compare the percentage of E/R$^+$ cells grown for 4 days under the indicated conditions vs the basal culture.

Supplementary Fig.6

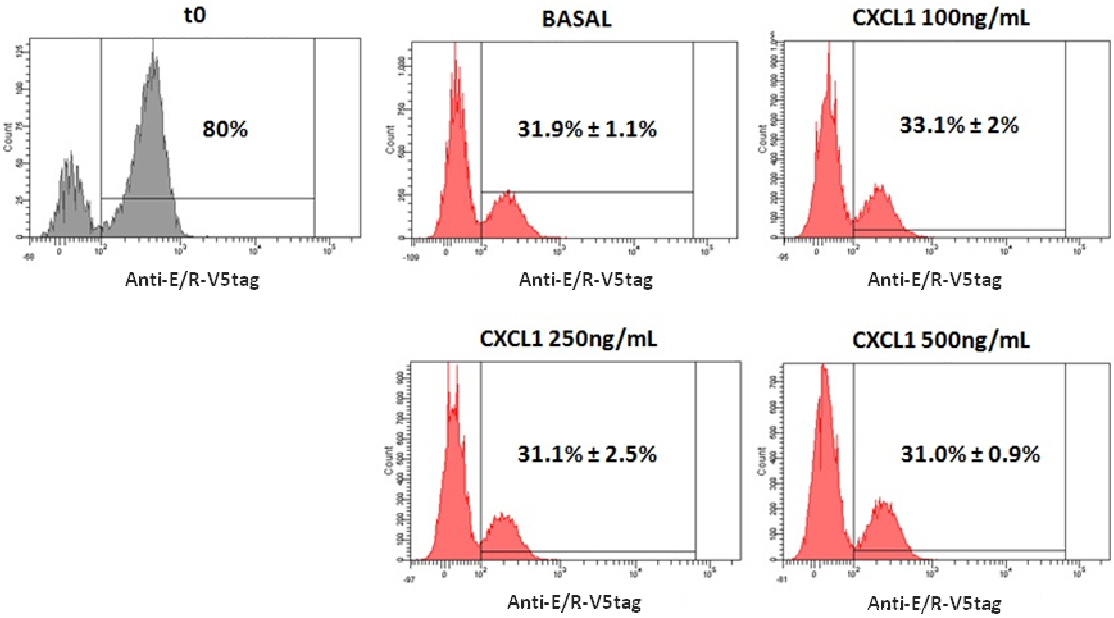

Fig.S6: CXCL1 does not provide a selective advantage to E/R^{+} Ba/F3 in competitive liquid culture. Control and E/R^{+} Ba/F3 were mixed at a starting ratio of 20%:80% and cultivated for 4 days in standard liquid culture in the absence (basal condition) or presence of increasing doses of recombinant murine CXCL1. Peaks are from a representative experiment, whereas values indicate mean±SD of 3 independent experiments.

Supplementary Fig.7

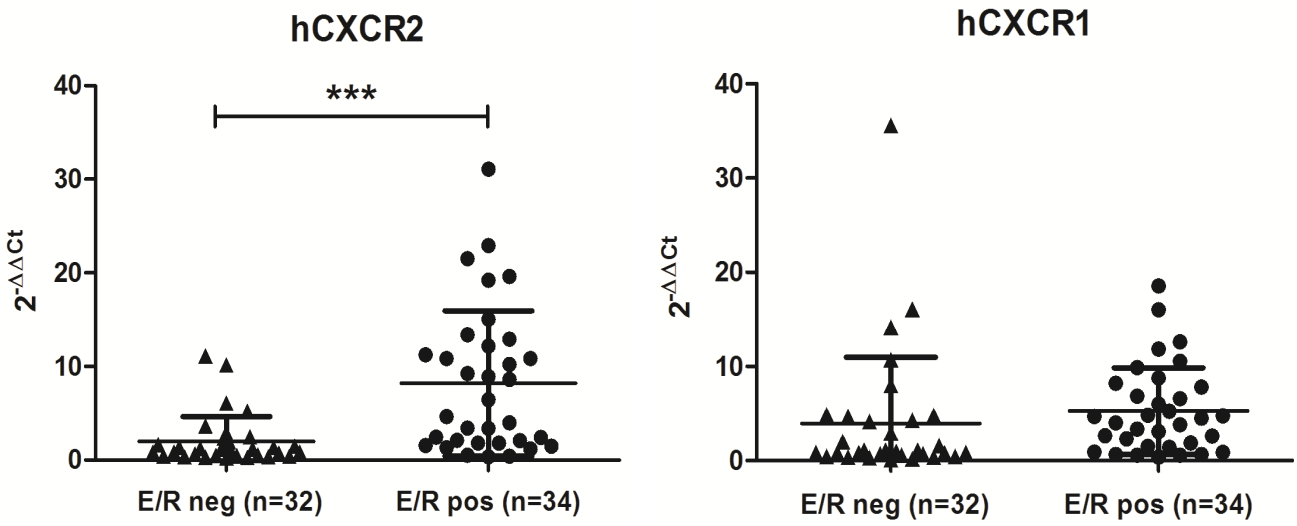

Fig.S7: E/R^{+} BCP-ALL patients overexpress CXCR2 mRNA compared BCP-ALL patients negative for all common translocations. cDNA of primary blasts of E/R-positive and negative BCP-ALL patients was subjected to RT-qPCR to quantify expression of CXCR2 and CXCR1. The median DeltaCt of negative E/R patients was considered as internal reference for fold change calculation. Student's t-test: ***, *p<0.001*. Patients characteristics are provided in **Supplementary Table 3.**

Supplementary Fig.8

A

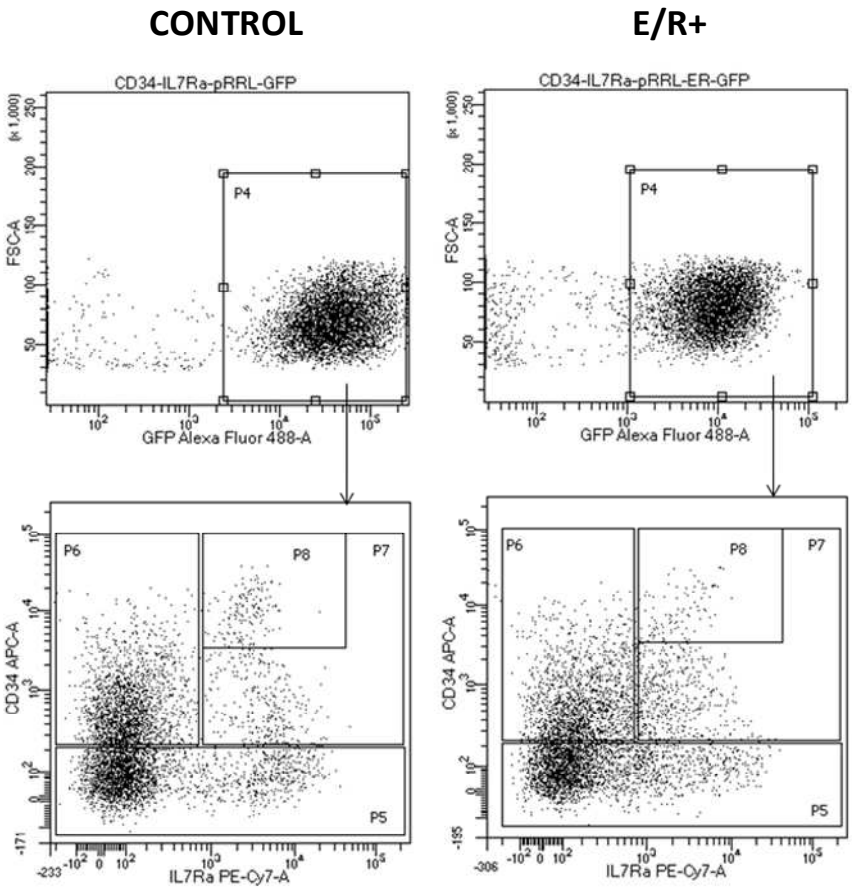

B

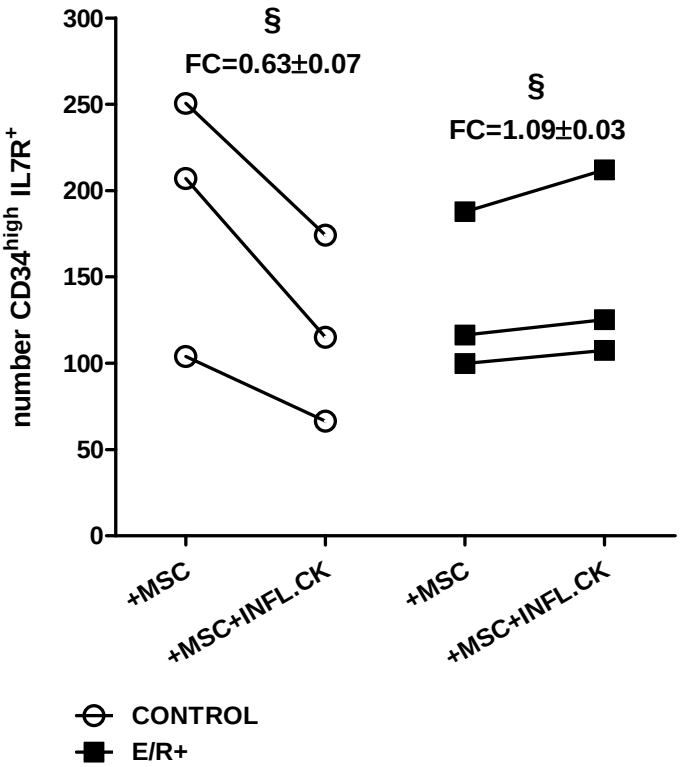

Fig.S8: A) Representative plots for relative quantitative analysis of the $CD34^-$, $CD34^+IL7R^-$, $CD34^+IL7R^+$ and $CD34^{high}IL7R^+$ fractions within control and pre-leukemic GFP^+ populations. Control and E/R-transduced UCB-$CD34^+$ cells were separately grown in stem culture medium on BM-MSC, in absence (+MSC) or presence of IL6/TNFα/IL1β (+MSC+INFL.CK) for 72h. At the end of the culture, cells were stained with APC-conjugated anti-hCD34 and PE-Cy7-conjugated anti-hIL7R antibodies and analyzed by quantitative flow-cytometry. Plots show a representative phenotypic analysis of both cell groups after the cultivation on unstimulated BM-MSC. P4 = GFP^+ population; P5 = $CD34^+IL7R^+$; P6 = $CD34^+IL7R^-$; P7 = $CD34^-$; P8 = $CD34^{high}IL7R^+$. **B) Human E/R^+ $CD34^{high}IL7R^+$ progenitors are preserved under mesenchymal inflammation.** Control and E/R-transduced UCB-$CD34^+$ cells were separately grown in stem culture medium on BM-MSC, in absence (+MSC) or presence of IL6/TNFα/IL1β (+MSC+INFL.CK) for 72h. At the end of the culture, cells were stained with the anti-hCD34 and anti-hIL7Rα antibodies and number of cells quantified by FACS. The cell number was normalized on a determined number of fluorescent reference beads (BD Trucount® tubes) and percentage of GFP positivity in the two groups. The graph shows results of one infection experiment in which cells were cultivated on three different healthy donor-derived BM-MSC monolayers. For every BM-MSC healthy donor, FC between the number of $CD34^{high}IL7R^+$ in the inflamed and unstimulated BM-MSC niche was calculated and the mean±SD indicated in the graph. One-sample t-test: §, $p<0.05$.

SUPPLEMENTARY MATERIALS

- **Ba/F3 gene expression profile**

E/R induction experiments showing >90% viability and FITC positivity were chosen for total RNA extraction by RNeasy Mini Kit (QIAGEN, Venlo, The Netherlands). Gene Chip Mouse 2.0 Arrays (Affymetrix) were used and data (.CEL files) generated using default Affymetrix microarray analysis parameters (Command Console suite software, Affymetrix). Gene ontology (GO) analysis was performed by expressing raw data in linear fold change and submitted them to Metascape (http://metascape.org). Differentially expressed genes were identified using Significance Analysis of Microarray algorithm (SAM) coded in the *samr* R package[1]. In SAM, we estimated the percentage of false positive predictions (i.e., False Discovery Rate, FDR) with 100 permutations. In the dendogram representation the 20 best *p-values* were used.

- **Analysis of competitive murine mesenchymal niche experiments**

After 4 days of co-culture, cells were harvested and stained with Horizon^{TM} Fixable Viability Stain 450 (BD Bioscience) and a PE-conjugated anti-mCD45 antibody (eBioscience, San Diego, CA, USA) to identify viable Ba/F3 cells. Cells were then fixed/permeabilized (BD Cytofix/Cytoperm Kit, BD Bioscience) and stained with a FITC-conjugated anti-V5tag antibody. Cells were analyzed by BD Bioscience FACSCanto-II. The percentage of FITC^{+} cells was evaluated by gating on Horizon480^{-}/mCD45^{+} cells and data were analyzed by FACSDiva software (BD Bioscience).

- **Quantitative Reverse Transcription PCR (RT-qPCR)**

Real-time quantification of gene transcripts was performed by the Light Cycler 480II instrument (Roche Diagnostics, Basel, Switzerland) using the Universal Probe Master System (Roche Diagnostics). Optimal primers and probe for cDNA amplification were selected by the Roche ProbeFinder software (https://www.roche-appliedscience.com/sis/rtpcr/upl). Data were expressed using the comparative 2_DDCt method[2] using *Hprt* as reference gene in case of Ba/F3. Transcript levels in pre-leukemic cells were always referred to those of control cells. For *Cxcr1/2* gene expression on primary blasts, 66 BCP-ALL patients, enrolled in the AIEOP-BFM ALL 2009 protocol and treated in AIEOP Centers, were included in the study. The protocol was approved by the Institutional Review Board (AIEOP-BFM ALL 2009 protocol; EudraCT-2007-004270-43). Thirty-two patients were E/R positive while 34 patients were negative for all common chromosomal translocations. The clinical characteristics of patients are shown in **Supplementary Table 3**. RNA was isolated from mononuclear cells, and cDNA was synthesized according to standard methods. Transcripts levels were normalized with respect to human *Gus* gene. The median of DeltaCt value of untranslocated patients was used as reference for fold change calculation.

- **Murine CXCR1/2 immunostaining**

Surface expression of CXCR1/2 in Ba/F3 was evaluated by staining cells with PE-conjugated anti-CXCR2 (BioLegend, San Diego, CA, USA) and anti-CXCR1 (R&D System, Minneapolis, MN, USA) for 30 min at +4°C. Cells were then acquired through BD Bioscience FACSCanto-II and data analyzed by FACSDiva software (BD Bioscience, San Jose, CA, USA).

- **BM-MSC derivation and culture**

Murine bone marrow mesenchymal stromal cells (BM-MSC) were isolated and characterized as previously described[3]. A well-established murine primary line was cultured in low glucose DMEM (Euroclone), 20% tested FBS (Hyclone), 1% L-Glut, 1% P/S and used for experiments between passage 8 (P8) and 11 (P11). Human BM-MSC were isolated from healthy donors BM aspirates, characterized and cultured as previously described[4]. Only cells between passages 3 (P3) and 5 (P5) were used.

- **Enzyme-linked immunosorbent assays (ELISA) and protein arrays**

For inflammatory stimulation of human BM-MSC, IL6 (40ng/ml), TNFα (100ng/ml) and IL1β (50ng/ml) (all from Immunotools, Friesoythe, Germany) were used[5]. Supernatants were collected after 24h, centrifuged 10min at 1260rcf and frozen at -80°C. Supernatants were analyzed by Human Cytokines Array C1000 (RayBio, Norcross, GA, USA) following the manufacturer's protocol and data were acquired by UVITEC Cambridge® instrument. Densitometry analysis was performed with ImageJ® software. For the inflammatory stimulation of murine BM-MSC, IL6 (20ng/ml), TNFα (50ng/ml) and IL1β (25ng/ml) (all from Immunotools) were used[3]. Murine KC and murine TGFβ DuoSet Enzyme-Linked Immunosorbent Assays (ELISA) (R&D Systems) were used following the manufacturer's protocols and plates were acquired by TECAN GENios® instrument.

- **Migration assay**

Control and E/R$^+$ Ba/F3 cells ($3x10^5$) were resuspended in 100µL of migration medium (Advanced RPMI, 2% FBS, 1% L-glutamine) and loaded into the upper chamber of 8.0µm Transwells©; murine BM-MSC supernatant (600 µl) was added to the lower chamber. Murine BM-MSC supernatants were specifically produced by maintaining cells in migration medium for 48h, in the presence or not of rmIL6 (20ng/mL), rmIL1β (25ng/mL) and

rmTNFα (50ng/mL) and frozen at -80°C. SB-265610 (1µM) was used for the specific inhibition of CXCR2; in this case, cells were pretreated for 10min at 37°C prior to be loaded into Transwells®. After 3h of migration at 37°C, 5% CO_2, Transwells® were removed, the migrated cells recovered and counted by flow-cytometry. A determined number of fluorescent reference beads (BD Trucount® tubes) were added to the tubes and used as internal calibrators. Cells were counted in technical triplicates for 30sec. The percentage of migrated cells was determined by dividing the number of cells in the lower chamber by the number of cells loaded into the upper chamber (input).

- **Cell cycle analysis**

Control and E/R^+ Ba/F3 ($0.5x10^6$) were stained with 2.5µM carboxyfluorescein succinimidyl ester (CFSE); $2.5x10^4$ stained cells were then mixed (20%ctr:80%E/R^+) and cultured into 6-well plates for 4 days in basal condition or on murine BM-MSC in the presence or absence of inflammatory cytokines. At the end of the culture, cells were harvested and stained with PE anti-mCD45 antibody. Cells were then fixed/permeabilized and stained with the primary anti-E/R fusion antibody (clone 6F2) (Merck Millipore, Burlington, MA, USA) and the secondary BD Horizon BV421 goat anti-rat IgG (BD Bioscience) in place of the FITC-conjugated anti-V5 antibody. Cells were then analyzed by flow cytometry to determine CFSE MFI. CFSE MFI of control Ba/F3 in basal condition was considered as referrer value for the fold increase calculation. Since cells dilute CFSE at each cell-cycle, proliferation rate and CFSE MFI are inversely correlated.

- **Apoptosis assay**

A mix of control and E/R^+ Ba/F3 (20%ctr:80%E/R^+; $2.5x10^4$ total cell number) were cultured into 6-well plates for 4 days in basal condition or on murine BM-MSC in the

presence or absence of inflammatory cytokines. At the end of the culture, cells were harvested and stained with BV650-conjugated anti-murine CD45 antibody and with Annexin V-Enzo Gold (enhanced Cyanine 3) (GFP-Certified Apoptosis/Necrosis Detection Kit, Enzo Life Sciences, Farmingdale, NY, USA). Cells were then fixed/permeabilized and stained with FITC-conjugated anti-V5 antibody. For each condition, percentage of $BV650^{+}$/Enzo $Gold^{-}$ cells was evaluated.

- **Human UCB-$CD34^{+}$ cells isolation and transfection**

Human umbilical cord blood (UCB)-derived $CD34^{+}$ cells were obtained from volunteer mothers receiving informed consent (BM-Niche Protocol, approved by the "Comitato etico della provincia Monza Brianza"). UCB mononuclear cells were separated by Ficoll-Paque PLUS (GE Healthcare, Chicago, IL, United States) within 24h from collection and immunomagnetic separation was performed on column using the CD34 MicroBead Kit (MACS Miltenyi Biotec, Bergisch Gladbach, North Rhine-Westphalia, Germany). The previously described E/R myc-tag fusion construct[6] was subcloned into the PmeI site of pRRL-EF1α-PGK-GFP dual-promoter plasmid. Vesicular stomatitis virus-G-pseudotyped viral particles were generated on 293T cells by polyethylenimine (PEI, Polysciences, Warrington, PA, USA) transfection and concentrated by ultracentrifugation. In details, 293T cells were plated in 6-well plates ($4x10^{6}$) in high glucose DMEM supplemented with pyruvate (Euroclone) and added with 10% tested FBS (HyClone), 1%L-Glut, 1% P/S, 1% non-essential aminoacids (Sigma-Aldrich, Saint Louis, MO, USA) until reaching about 80% confluence after 24h. Transfection mixes were prepared as follows: 500μL high glucose DMEM, 4μg psPAX2 packaging vector, 2μg VSV-G envelope vector, 8μg pRRL-GFP (empty vector, EV) or pRRL-E/R-GFP (E/R), 35μg 25kDa linear PEI. After 48h and 72h, cell supernatants were collected, 0.45μm filtered and ultracentrifuged at 26.000rpm for

2.5h at +4°C. UCB-CD34^{+} cells (2x10^{6}) were infected for 72h with concentrated viruses in StemSpam SFEM-II (StemCell) supplemented with SCF (100 ng/mL), FLT3 ligand (100 ng/mL), and IL-3 (10 ng/mL) (all from PeproTech) and polybrene (1µg/mL; Sigma-Aldrich). After 72h of infection, GFP^{+} cells within pRRL-GFP and pRRL-E/R-GFP populations were sorted (purity >95%) and maintained in stem culture medium (StemSpam SFEM-II (supplemented with 100 ng/mL SCF, 100 ng/mL FLT3-ligand, 10 ng/mL IL-3, 20ng/mL IL6 and 50ng/mL TPO).

- **Analysis of transduced UCB-CD34^{+} and BM-MSC co-cultures**

At the end of the co-culture (72h), cells were collected and stained for 30min at +4°C with APC-conjugated anti-human CD34 (BD Biosciences) and Pe-Cy7-conjugated anti-human CD127 (IL7R) (BioLegend) antibodies. Cells were acquired through BD Bioscience Fortessa, and data analyzed by FACSDiva software (BD Bioscience). A known number of fluorescent reference beads (BD Trucount tubes, BD Bioscience) were added into the FACS tube prior to counting the cells in technical duplicates for 60sec. Cells number was normalized on counted beads and percentage of the GFP^{+} fraction.

- **γH2AX staining**

A mix of control and E/R^{+} Ba/F3 (20%ctr:80%E/R^{+}; 2.5x10^{4} total cell number) were cultured in 6-well plates for 4 days in basal condition or on murine BM-MSC in the presence or absence of inflammatory cytokines. At the end of the culture, cells were harvested and stained (0.5-1x10^{6}) with Horizon® Fixable Viability Stain 450, fixed 10min at 37°C in 4% formaldehyde and permeabilized in 90% methanol. After 30min incubation on ice, cells were firstly stained with PE anti-CD45 and then with Alexa Fluor® 647-anti-

Phospho-Histone H2A.X Ser139 (20E3) and with FITC anti-V5 antibodies. Alexa Fluor® 647- Rabbit (DA1E) mAb IgG XP® was used as isotype control (Cell Signalling).

References

1 Tusher VG, Tibshirani R, Chu G. Significance analysis of microarrays applied to the ionizing radiation response. *Proc Natl Acad Sci* 2001; **98**: 5116-21.

2 Livak KJ, Schmittgen TD. Analysis of relative gene expression data using real-time quantitative PCR and the 2-ΔΔCT method. *Methods* 2001; **25**: 402-8.

3 Cappuzzello C, Doni A, Dander E, Pasqualini F, Nebuloni M, Bottazzi B *et al.* Mesenchymal stromal cell-derived PTX3 promotes wound healing via fibrin remodeling. *J Invest Dermatol* 2016; **136**: 293-300.

4 Bardelli D, Dander E, Bugarin C, Cappuzzello C, Pievani A, Fazio G *et al.* Mesenchymal stromal cells from Shwachman-Diamond syndrome patients fail to recreate a bone marrow niche in vivo and exhibit impaired angiogenesis. *Br J Haematol* 2018; **182**: 114-24.

5 Portale F, Cricrì G, Bresolin S, Lupi M, Gaspari S, Silvestri D *et al.* ActivinA: a new leukemia-promoting factor conferring migratory advantage to B-cell precursor-acute lymphoblastic leukemic cells. *Haematologica* 2018; epub ahead of print.

6 Ford AM, Palmi C, Bueno C, Hong D, Cardus P, Knight D *et al.* The TEL-AML1 leukemai fusion gene dysregulates the TGF-beta pathway in early B lineage progenitor cells. *J Clin Invest* 2009; **119**: 826-36.